Composite scalar Dark Matter from vector-like $SU(2)$ confinement

Roman Pasechnik,[1] Vitaly Beylin,[2] Vladimir Kuksa,[2] and Grigory Vereshkov[2,3]

[1] *Department of Astronomy and Theoretical Physics, Lund University, SE-223 62 Lund, Sweden*
[2] *Research Institute of Physics, Southern Federal University, 344090 Rostov-on-Don, Russia*
[3] *Institute for Nuclear Research of Russian Academy of Sciences, 117312 Moscow, Russia*

A toy-model with $SU(2)_{\rm TC}$ dynamics confined at high scales $\Lambda_{\rm TC} \gg 100$ GeV enables to construct Dirac UV completion from the original chiral multiplets predicting a vector-like nature of their weak interactions consistent with electroweak precision tests. In this work, we investigate a potential of the lightest scalar baryon-like (T-baryon) state $B^0 = UD$ with mass $m_B \gtrsim 1$ TeV predicted by the simplest two-flavor vector-like confinement model as a Dark Matter (DM) candidate. We show that two different scenarios with the T-baryon relic abundance formation before and after the electroweak (EW) phase transition epoch lead to symmetric (or mixed) and asymmetric DM, respectively. Such a DM candidate evades existing direct DM detection constraints since its vector coupling to Z boson absents at tree level, while one-loop gauge boson mediated contribution is shown to be vanishingly small close to the threshold. The dominating spin-independent (SI) T-baryon–nucleon scattering goes via tree-level Higgs boson exchange in the t-channel. The corresponding bound on the effective T-baryon–Higgs coupling has been extracted from the recent LUX data and turns out to be consistent with naive expectations from the light technipion case $m_{\tilde{\pi}} \ll \Lambda_{\rm TC}$. The latter provides the most stringent phenomenological constraint on strongly-coupled $SU(2)_{\rm TC}$ dynamics so far. Future prospects for direct and indirect scalar T-baryon DM searches in astrophysics as well as in collider measurements have been discussed.

PACS numbers: 95.35.+d, 98.80.-k, 95.30.Cq, 14.80.Tt
Keywords: Dark Matter candidates; Dark Matter annihilation; Dark Matter direct detection; low-energy effective field theories; Technicolor; technibaryon

arXiv:1407.2392v2 [hep-ph] 16 Mar 2016

I. INTRODUCTION

After recent discovery of the Higgs boson [1, 2] at the LHC and follow-up precision studies of its interactions with known matter [3], a rough picture of consistency with the Standard Model (SM) has began to emerge. The SM is being widely perceived as an effective field theory providing quite accurate results and matches the physical reality at low energies to a rather high precision. So the observed consistency does not mean yet that the nature of the Higgs boson and electroweak symmetry breaking (EWSB) is completely understood at the fundamental level. One of the immediate questions that challenge our current understanding of symmetries in Nature is what initiates the Higgs mechanism of electroweak symmetry breaking (EWSB) in the SM. Namely, whether it is actually SM-like or in fact an effective description appearing as a consequence of a new fundamental symmetry. The experimental precision in the Higgs SM sector should be noticeably increased to the level of precision tests achieved in other SM sectors (i.e. flavor and electroweak (EW) gauge boson sectors) in order to draw final conclusions. In particular, in the EW sector of the SM the agreement of theoretical predictions with precision measurements takes place at the level of $\sim 10^{-3}$ in relative error which remains a rather big challenge for ongoing experimental investigations of the SM Higgs sector at the LHC.

A new strongly-coupled dynamics at a TeV energy scale is often considered to be responsible for EWSB in the SM [5–8]. Namely, it initiates the EWSB dynamically by means of strongly-interacting techniquark (or T-quark) condensation at low energy scales ~ 100 GeV. A straightforward analogy to this effect is the spontaneous chiral symmetry breaking in non-perturbative chiral QCD with only difference that the effective Higgs mechanism is initiated by a non-diagonal T-quark condensate. Such a new dynamics unavoidably predicts a plenty of new states, most importantly, composite Higgs-like particles [11, 12] and partners of SM fermions [13], whose properties depend on the group-theoretical structure of underlined theory and its ultraviolet (UV) completion. Besides the composite Higgs-like state, the latter predict a plenty of new relatively light pseudo-Goldstone composite states, like technipions (or T-pions below), techni-η, techni-K, etc, whose search in low invariant mass regions is strongly limited by large SM backgrounds and weak couplings to SM particles. The search for a family of new light (pseudo)scalar states with invariant masses below 200 GeV is one of the priority topics for new strongly-coupled physics searches at the LHC Run II.

A large number of various realisations of such a new dynamics at a TeV scale, commonly dubbed as "Technicolor" (TC) or "compositeness" scenarios, have been proposed in the literature so far (for a review, see e.g. Refs. [9, 10]). Such a big variety, however, has got reduced by severe electroweak (EW) precision tests [14, 15] and recent SM Higgs-like particle observations. At present, among the most appealing scenarios of dynamical EWSB consistent with current constraints is a class of models with vector-like (Dirac) UV completion – the vector-like confinement (VLC) scenario. The phenomenological importance of the vector-like confinement

has been broadly discussed in e.g. Ref. [16] without referring to its implication to the dynamical EWSB. The simplest realisation of the VLC scenario of the EWSB with two vector-like or Dirac techniflavors and a SM-like Higgs boson has been studied in Refs. [17–19] and very recently has emerged in composite Higgs scenarios with confined $SU(2)_{\rm TC}$ [20, 21]. In this paper, we discuss implications of the vector-like confinement to Dark Matter (DM) astrophysics.

Besides the dynamical nature of EWSB in the SM and a possible compositeness of the Higgs boson, another very important prediction of QCD-like TC scenarios based upon $SU(N_{\rm TC})_{\rm TC}$ confined symmetry is the existence of heavy composite baryon-like states possessing an additional conserved quantum number. The lightest neutral technibaryon (or T-baryon) state thus appears to be stable and weakly interacting with ordinary matter. If a new strong dynamics exists in Nature just above the EW scale $M_{\rm EW} \simeq 200$ GeV and if there is a mechanism for T-baryon asymmetry generation analogical to that of baryon asymmetry, such new particles could be abundantly produced in early Universe and survived until today in the form of DM [23]. These ideas is widely discussed in the literature during past two decades.

So far, a number of different models of composite DM candidates and hypotheses about their origin and interactions has been proposed. Generic DM signatures from TC-based models with stable T-baryons were discussed e.g. in Refs. [24–28] (for a review see also Ref. [29] and references therein). In particular, well-known minimal dynamical EWSB mechanisms predict relatively light T-baryon states as pseudo Nambu-Goldstone bosons of the underlying gauge theory [30, 31, 33]. The latter can naturally provide partially-asymmetric or asymmetric DM (ADM) candidates if one assumes the existence of a T-baryon asymmetry in Nature similarly to ordinary baryon asymmetry [31, 33] (for a review on ADM models, see e.g. Ref. [34] and references therein). Having similar mechanisms for ordinary matter and DM formation in early Universe one would expect the DM density to be of the same order of magnitude as that of baryons. Depending on a particular realization of dynamical EWSB mechanism such composite DM candidates may be self-interacting which helps in avoiding problematic cusp-like DM halo profiles [35]. The ongoing search for the DM in both direct and indirect measurements can thus provide further tight constraints on possible TC scenarios additional to those coming from the LHC.

To this end, in Ref. [18] it has been demonstrated explicitly that the TC scenarios with an odd confined $SU(2n+1)_{\rm TC}$, $n = 1, 2, \ldots$ symmetry are most likely ruled out by recent constraints on the spin-independent DM-nucleon scattering cross section [36, 37]. In particular, stable Dirac T-neutron DM predicted by the confined QCD-like $SU(3)_{\rm TC}$ symmetry is excluded due to its large tree-level vector gauge coupling to the Z boson unless it is not directly coupled to weak isospin $SU(2)_{\rm W}$ sector, only via a small mixing.

However, confined even $SU(2n)_{\rm TC}$, $n = 1, 2, \ldots$ symmetries giving rise to scalar T-baryon $B = QQ$ (diquark-like) states instead are void of this problem. Indeed, the elastic scattering of scalar T-baryons off nucleons occurs mainly via the Higgs boson exchange at tree level and is strongly suppressed compared to stable Dirac composites. As was advocated recently in Refs. [31, 32] the *light* scalar T-baryons (or T-diquarks) can play a role of pseudo-Goldstone bosons under global $SU(4)$ symmetry such that the lightest neutral UD T-baryon state could become a new appealing composite asymmetric or mixed DM candidate. In this Letter, we are focused primarily on a simpler *global chiral* $SU(2)_L \otimes SU(2)_R$ symmetry acting on complex vector-like (Dirac) UV completion in *local gauge* $U(1)_{\rm Y} \otimes SU(2)_{\rm W} \otimes SU(2)_{\rm TC}$ symmetry which possesses an additional conserved T-baryon charge [17–19]. Continuing earlier line of studies, now we discuss important phenomenological implications of *heavy* scalar T-baryons $m_B \gtrsim 1$ TeV for direct DM searches in astrophysics and collider measurements. Specifically, we demonstrate that the heavy scalar T-baryon is a good candidate for self-interacting *symmetric* DM which is within a projected few-year reach at direct detection experiments.

II. SCALAR T-BARYON INTERACTIONS

A. Vector-like confinement and Dirac T-quarks

In the considering version of the model, the large scalar T-baryon mass terms explicitly break global chiral $SU(4)$, so in this case it suffices to work within the global chiral $SU(2)_{\rm R} \otimes SU(2)_{\rm L}$ symmetry which classifies the lightest TC states only, similarly to that in hadron physics. This in variance with models of Refs. [31, 32] where the pseudo-Goldstone T-baryon states can be arbitrarily light and are typically considered to be around the electroweak scale.

Consider the simplest vector-like TC model with single $SU(2)_{\rm W}$ doublet of Dirac T-quarks confined under a new strongly-coupled gauge symmetry $SU(N_{\rm TC})_{\rm TC}$ at the T-confinement scale $\Lambda_{\rm TC} \gtrsim 1$ TeV

$$\tilde{Q} = \begin{pmatrix} U \\ D \end{pmatrix}, \qquad Y_{\tilde{Q}} = \begin{cases} 0, & \text{if } N_{\rm TC} = 2\,, \\ 1/3, & \text{if } N_{\rm TC} = 3\,. \end{cases} \tag{2.1}$$

where the T-quark doublet hypercharges are chosen to provide integer-valued electric charges of corresponding bounds states. The case of $N_{\rm TC} = 3$ has been studied in Refs. [17, 18], and here we are focused primarily on $N_{\rm TC} = 2$ theory where phenomenologically consistent vector-like weak interactions of an underlined UV completion (i.e. Dirac T-quarks) can be naturally obtained from a conventional chiral one (for $N_{\rm TC} = 3$ this is not the case).

In order to demonstrate this fact explicitly, let us start with two generations ($A = 1, 2$) of left-handed T-quarks

$Q^{a\alpha}_{L(A)}$ transformed under gauge $SU(2)_{\rm W}\otimes SU(2)_{\rm TC}$ as

$$\begin{aligned}\tilde{Q}^{a\alpha'}_{L(A)} &= \tilde{Q}^{a\alpha}_{L(A)} + \frac{i}{2}g_W\theta_k\tau_k^{ab}\tilde{Q}^{b\alpha}_{L(A)}\\ &+\frac{i}{2}g_{TC}\varphi_k\tau_k^{\alpha\beta}\tilde{Q}^{a\beta}_{L(A)}\,,\end{aligned} \tag{2.2}$$

where $a=1,2$ is the index of fundamental representation of weak isospin $SU(2)_{\rm W}$ group, $\alpha=1,2$ in the index of fundamental representation of T-strong $SU(2)_{\rm TC}$, and $Y_{\tilde{Q}}=0$. Now, let us keep the first generation of T-quarks unchanged and apply the charge conjugation to the second generation such that

$$\begin{aligned}\hat{\mathbf{C}}Q^{a\alpha}_{L(2)} &= Q^{Ca\alpha}_{L(2)}\,,\\ Q^{Ca\alpha'}_{L(2)} &= Q^{Ca\alpha}_{L(2)} - \frac{i}{2}g_W\theta_k(\tau_k^{ab})^*Q^{Cb\alpha}_{L(2)}\\ &-\frac{i}{2}g_{TC}\varphi_k(\tau_k^{\alpha\beta})^*Q^{Ca\beta}_{L(2)}\,.\end{aligned} \tag{2.3}$$

The charge conjugation of a chiral fermion changes its chirality. This fact enables us to define the corresponding right-handed field as

$$Q^{a\alpha}_{R(2)} \equiv \varepsilon^{ab}\varepsilon^{\alpha\beta}Q^{Cb\beta}_{L(2)}\,,\quad \varepsilon^{ab}=\varepsilon^{\alpha\beta}=\begin{pmatrix}0&1\\-1&0\end{pmatrix}\,. \tag{2.4}$$

Starting from the gauge group transformation property (2.3) and applying $SU(2)$ defining relations like $\delta^{ab}=\varepsilon^{ac}\varepsilon^{bc}$ and

$$\varepsilon^{ab}(\tau_k^{bc})^*\varepsilon^{cf}=\tau_k^{af},\qquad \varepsilon^{\alpha\beta}(\tau_k^{\beta\gamma})^*\varepsilon^{\gamma\mu}=\tau_k^{\alpha\mu}\,,$$

it is rather straightforward to show that

$$\begin{aligned}Q^{a\alpha'}_{R(2)} &= Q^{a\alpha}_{R(2)} + \frac{i}{2}g_W\theta_k\tau_k^{ab}Q^{b\alpha}_{R(2)}\\ &+\frac{i}{2}g_{TC}\varphi_k\tau_k^{\alpha\beta}Q^{a\beta}_{R(2)}\,.\end{aligned} \tag{2.5}$$

By a comparison of Eq. (2.5) with Eq. (2.2) one notices that the transformation properties of the *right-handed* T-quark field obtained by charge conjugation and transposition of the left-handed field of the *second* generation coincide with the transformation properties of the *left-handed* field of the *first* generation. Therefore, starting initially with two chiral (left-handed) T-quark generations we arrive at *one vector-like generation of (Dirac) T-quarks*, namely

$$Q^{a\alpha}=Q^{a\alpha}_{L(1)}+Q^{a\alpha}_{R(2)}=Q^{a\alpha}_{L(1)}+\varepsilon^{ab}\varepsilon^{\alpha\beta}Q^{Cb\beta}_{L(2)}\,. \tag{2.6}$$

As was argued for the first time in Ref. [17], practically any simple Dirac UV completion with chirally-symmetric weak interactions easily evade the most stringent electroweak constraints which is the basic motivation for the VLC scenario.

The phenomenological interactions of the constituent Dirac T-quarks and the lightest T-hadrons, namely, the scalar SM-singlet T-sigma S field, and the $SU(2)_{\rm W}$-adjoint triplet of T-pion fields P_a, $a=1,2,3$, are described by the (global) chiral $SU(2)_{\rm R}\otimes SU(2)_{\rm L}$ invariant low-energy effective Lagrangian in the linear σ-model (LσM)

$$\begin{aligned}\mathcal{L}_{\rm L\sigma M} &= \frac{1}{2}\,\partial_\mu S\,\partial^\mu S+\frac{1}{2}D_\mu P_a\,D^\mu P_a + i\bar{\tilde{Q}}\hat{D}\tilde{Q}\\ &-g_{\rm TC}\bar{\tilde{Q}}(S+i\gamma_5\tau_a P_a)\tilde{Q}-g_{\rm TC}\,S\,\langle\bar{\tilde{Q}}\tilde{Q}\rangle\\ &-\lambda_{\rm H}\mathcal{H}^4-\frac{1}{4}\lambda_{\rm TC}(S^2+P^2)^2+\lambda\mathcal{H}^2(S^2+P^2)\\ &+\frac{1}{2}\mu_{\rm S}^2(S^2+P^2)+\mu_{\rm H}^2\mathcal{H}^2\,,\end{aligned} \tag{2.7}$$

with a particular choice of the "source" term linear in T-sigma where $\langle\bar{\tilde{Q}}\tilde{Q}\rangle<0$ is the diagonal T-quark condensate, $\mathcal{H}^2=\mathcal{H}\mathcal{H}^\dagger$, $P^2\equiv P_aP_a=\tilde{\pi}^0\tilde{\pi}^0+2\tilde{\pi}^+\tilde{\pi}^-$, and the EW-covariant derivatives are

$$\begin{aligned}\hat{D}\tilde{Q} &= \gamma^\mu\left(\partial_\mu-\frac{iY_{\tilde{Q}}}{2}\,g'B_\mu-\frac{i}{2}\,gW^a_\mu\tau_a\right)\tilde{Q}\,,\\ D_\mu P_a &= \partial_\mu P_a+g\epsilon_{abc}W^b_\mu P_c\,.\end{aligned} \tag{2.8}$$

The Higgs boson doublet $\mathcal{H}$ in Eq. (2.7) acquires an interpretation as a composite bound state of vector-like T-quarks e.g. in the model extended by an extra $SU(2)_{\rm W}$-singlet Dirac $\tilde{S}$ T-quark such that $\mathcal{H}=\tilde{Q}\bar{\tilde{S}}$ (for other possibilities, see also Refs. [20, 21]). Note, however that at the moment the question about a particular UV content of the Higgs boson doublet is not of primary importance for the effective low-energy description of scalar T-meson interactions described by the phenomenological LσM Lagrangian (2.7) and thus will not be further discussed here.

Note, the chiral symmetry implies the equality of constituent Dirac masses $M_U=M_D\equiv M_{\tilde{Q}}$ at tree level. In the limit of small current T-quark masses $m_{\tilde{Q}}$ compared to the constituent ones $M_{\tilde{Q}}$, i.e. $m_{\tilde{Q}}\ll M_{\tilde{Q}}\sim\Lambda_{\rm TC}$, in analogy to ordinary QCD the conformal symmetry is approximate such that the μ-terms can be suppressed $\mu_{S,H}\ll m_{\tilde{\pi}}$, which will be employed below throughout this work. Then the spontaneous EW and chiral symmetry breakings are initiated dynamically by the Higgs $v\simeq 246\,{\rm GeV}$ and T-sigma u vevs

$$\begin{aligned}\mathcal{H} &= \frac{1}{\sqrt{2}}\begin{pmatrix}\sqrt{2}i\phi^-\\ H+i\phi^0\end{pmatrix}\,,\quad \langle H\rangle\equiv v\,,\quad \langle S\rangle\equiv u\gtrsim v\,,\\ H &= v+hc_\theta-\tilde{\sigma}s_\theta\,,\qquad S=u+hs_\theta+\tilde{\sigma}c_\theta\,,\end{aligned} \tag{2.9}$$

respectively, by means of T-quark condensation, namely,

$$\begin{aligned}u &= \left(\frac{g_{\rm TC}\lambda_{\rm H}}{\delta}\right)^{1/3}|\langle\bar{\tilde{Q}}\tilde{Q}\rangle|^{1/3}\,,\\ v &= \left(\frac{|\lambda|}{\lambda_{\rm H}}\right)^{1/2}\left(\frac{g_{\rm TC}\lambda_{\rm H}}{\delta}\right)^{1/3}|\langle\bar{\tilde{Q}}\tilde{Q}\rangle|^{1/3}\,,\end{aligned} \tag{2.10}$$

and the T-pions acquire a mass

$$m^2_{\tilde{\pi}}=-\frac{g_{\rm TC}\langle\bar{\tilde{Q}}\tilde{Q}\rangle}{u}\,.$$

In the above expressions, $s_\theta\equiv\sin\theta$, $c_\theta\equiv\cos\theta$, $\delta=\lambda_{\rm H}\lambda_{\rm TC}-\lambda^2$, $g_{\rm TC}>0$ and $\lambda_H>0$. The minimal choice

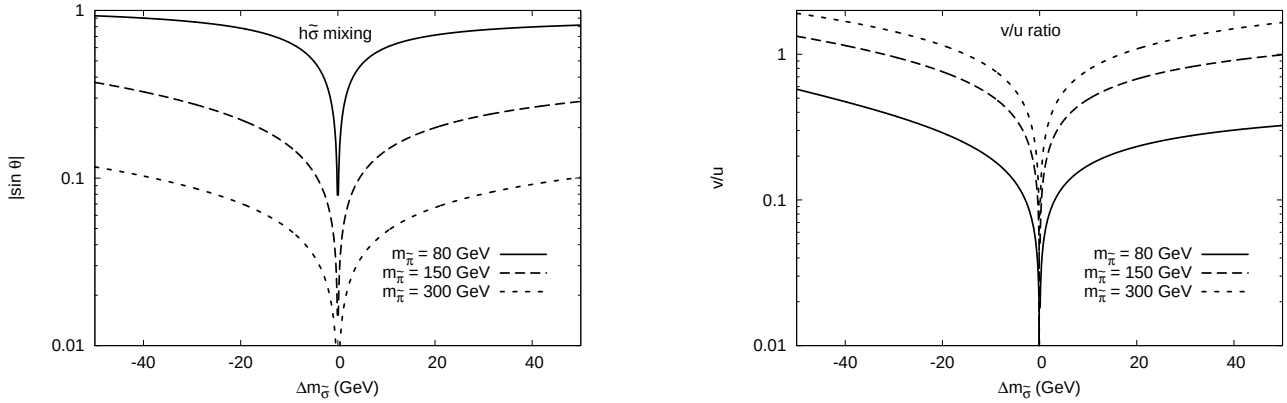

FIG. 1: The absolute value of sine of the $h\tilde{\sigma}$-mixing angle $|\sin\theta|$ (left) and the ratio of the chiral and EW breaking scales u/v (right) as functions of $\Delta m_{\tilde{\sigma}} \equiv m_{\tilde{\sigma}} - \sqrt{3}m_{\tilde{\pi}}$ for three different values of the T-pion mass $m_{\tilde{\pi}} = 80, 150$ and 300 GeV. Here and below, the nearly-conformal limit has been imposed.

of the "source" term in the LσM Lagrangian (2.7) is natural since it simultaneously (i) sets up a pseudo-Goldstone mass scale for T-pions, (ii) allows to link all the incident vevs u and v, and hence the constituent Dirac T-quark mass scale $M_{\tilde{Q}} = g_{\rm TC}u$, to the T-confinement scale, and (iii) describes the Yukawa interactions of the T-sigma with the diagonal T-quark condensate $\langle\bar{\tilde{Q}}\tilde{Q}\rangle$ which is the only dimensionfull nonperturbative parameter in the model at low energy scales. The Nambu-Goldstone d.o.f.'s $\phi^{\pm}, \phi^0$ originating from the Higgs doublet do not appear in the potential since $\mathcal{H}\mathcal{H}^{\dagger} = H^2/2$, where $\mathcal{H}$ and H are defined in Eq. (2.9). They, thus, can not mix with pseudoscalar T-pions and get absorbed by the gauge bosons in normal way giving rise to longitudinal polarisations of $W^{\pm}, Z$ bosons, respectively. So, T-pions do not have tree-level couplings to SM fermions, and can only be produced in vector-boson fusion channels [17, 19].

In the VLC approach, one could distinguish two natural physical scales associated with two chiral u and EW v symmetry breaking scales, which can, in principle, be very different from each other although are related to the single T-confinement scale, or the T-quark condensate $\langle\bar{\tilde{Q}}\tilde{Q}\rangle$. In a phenomenologically natural hierarchy $u \gg v$, the upper scale would then roughly be associated with the mass scale of constituent T-quarks and T-baryons, whereas the lower one – with the mass scale of lightest pseudo-Goldstone states, e.g. T-pions. By a convention, in effective field theory approach one would then consider only the lightest states ($\tilde{\pi}$, $\tilde{\sigma}$) which propagate at short distances and contribute to vacuum polarisations of the SM gauge bosons, while a net effect of all the heavy states (e.g. T-baryons, T-rho etc) can be effectively accounted for by constituent T-quark loops. This is a natural consequence of imposing an upper cut-off in loop momentum scale $\mu \sim \Lambda_{\rm TC} \sim M_{\tilde{Q}}$ in the low-energy effective description suitable for e.g. oblique corrections calculation [17].

In the framework of VLC model, the SM-like Higgs mechanism has an effective nature and is initiated by the Dirac T-quark condensation due to a presence of $\lambda\mathcal{H}^2S^2$ term in the potential (2.7). While the Peskin-Tacheuchi S and U parameters [14, 15] are strongly suppressed for all relevant model parameters $S, U \lesssim 0.01 - 0.001$, the T-sigma–Higgs mixing angle θ is bounded by the T-parameter and the SM Higgs decay constraints provided that $s_\theta \lesssim 0.2$ [17]. In general, such a phenomenologically consistent small $h\sigma$-mixing limit $s_\theta \to 0$ corresponds to a decoupling of the TC dynamics from the SM up to higher energy ~ 1 TeV scales, hence, to a suppressed ratio $v/u \ll 1$ as well as to relatively weak TC couplings $g_{\rm TC}, \lambda, \lambda_{\rm TC} \lesssim 1$ compared to analogical couplings in QCD. The latter property will be further employed in the T-baryon sector.

In Fig. 1 the dependencies of sine of the $h\tilde{\sigma}$-mixing angle $|s_\theta|$ (left panel) and the Higgs and T-sigma vevs v/u (right panel) on $\Delta m_{\tilde{\sigma}} \equiv m_{\tilde{\sigma}} - \sqrt{3}m_{\tilde{\pi}}$ are shown for three different T-pion mass values $m_{\tilde{\pi}} = 80, 150$ and 300 GeV. Consequently, in the case of small $s_\theta \to 0$ and $v/u \ll 1$, or equivalently, $\Delta m_{\tilde{\sigma}} \to 0$, the deviations of the Higgs properties from those in the SM are small while the dynamical nature of the Higgs mechanism as a theoretically favorable possibility is preserved. The physical Lagrangian of the VLC model can be found in Refs. [17, 19] and we do not repeat it here.

In the currently favorable phenomenological situation with the SM-like Higgs boson, what would be the basic phenomenological signature for dynamical EW symmetry breaking? Besides the light Higgs boson, in the VLC model described above the T-pions are among the lightest physical T-hadron states which should be searched for in vector boson VV and photon $\gamma\gamma$ fusion channels, preferably, in the low invariant mass region $m_{\tilde{\pi}} \sim 80{-}200$ GeV. The T-sigma state σ is expected to be somewhat heavier since the small Higgs–T-sigma mixing limit $s_\theta \ll 1$ corresponds to $m_\sigma \sim \sqrt{3}m_{\tilde{\pi}}$ (Fig. 1). Besides, the T-sigma interactions with gauge bosons are strongly suppressed. So, one of the most straightforward ways to search for the new strongly-coupled dynamics and dynamical EW

symmetry breaking in collider measurements is to look for T-pion signatures in $\gamma\gamma$-fusion channel [19].

Here, we discuss another source of constraints on such a new strong dynamics possibly coming from astrophysics measurements at direct DM detection experiments. For this purpose, let us consider the T-baryon spectrum of $SU(2)_{\rm TC}$ two-flavor theory.

B. Scalar T-baryon Lagrangian

Extra bound states of $SU(2)_{\rm TC}$ theory possessing an additional conserved (T-baryon) number analogous to the usual baryon number are given by scalar (anti)T-baryon multiplets Q_iQ_j and $\bar{Q}_i\bar{Q}_j$. As was previously studied in Refs. [31, 32], these states can play a role of pseudo-Goldstone bosons originating from global $SU(4)$ multiplets. In the phenomenologically relevant TC decoupling limit $u \ll v$ the T-baryons can have a large mass $m_B \gtrsim M_{\tilde{Q}} \gg m_{\tilde{\pi}}, m_H$ significantly exceeding the EW breaking scale. In this case, just above the EW scale one should employ the global chiral $SU(2)_L \otimes SU(2)_R$ symmetry in the T-meson sector whose effective Lagrangian is supplemented by an additional phenomenological SM-group invariant Lagrangian of heavy T-baryons. This case has not been discussed in the literature and deserves a special attention. And this is in variance with other somewhat similar UV completions not participating in the dynamical EW symmetry breaking such as those in Ref. [22].

In order to describe consistently the EW and effective interactions of scalar T-baryons, let us start with two real adjoint (composite) representations of the SM $SU(2)_{\rm W}$ gauge group G_a and F_a, $a = 1, 2, 3$, i.e. transforming in the weak basis as

$$G'_a = G_a - g\epsilon_{abc}\theta^b G_c\,, \quad F'_a = F_a - g\epsilon_{abc}\theta^b F_c\,. \tag{2.11}$$

Introducing a complex adjoint representation B with the unit T-baryon charge and $Y_{\rm B} = 0$ such as

$$\begin{aligned} B_a &= \frac{1}{\sqrt{2}}(G_a + iF_a)\,, \quad B^*_a \equiv \bar{B}_a \neq B_a\,, \\ B'_a &= B_a - g\epsilon_{abc}\theta^b B_c\,, \end{aligned} \tag{2.12}$$

one ends up with the gauge interactions of the scalar T-baryons B_a set by the corresponding covariant derivative

$$D_\mu B_a = \partial_\mu B_a + g\epsilon_{abc}W^b_\mu B_c\,. \tag{2.13}$$

In the charge basis, the physical T-baryon states are

$$B^\pm = \frac{B_1 \mp iB_2}{\sqrt{2}}\,, \quad \bar{B}^\pm = \frac{\bar{B}_1 \pm i\bar{B}_2}{\sqrt{2}}\,, \quad B^0 = B_3\,. \tag{2.14}$$

Desirably, these states now have a definite partonic representation as diquark–like bound states of U, D T-quarks with conserved T-baryonic number T_B, namely,

$$\begin{aligned} &B^+ = UU\,, \quad B^- = DD\,, \quad B^0 = UD\,, \quad T_B = +1\,, \\ &\bar{B}^+ = \bar{U}\bar{U}\,, \quad \bar{B}^- = \bar{D}\bar{D}\,, \quad \bar{B}^0 = \bar{U}\bar{D}\,, \quad T_{\bar{B}} = -1\,. \end{aligned}$$

For simplicity, at the first step in this work we assume that energetically favored states for such composites are the ones with $J = 0$, although the lightest state with $J = 1$ is not completely excluded and will be studied elsewhere. The low-energy effective Lagrangian of T-baryon interactions with SM gauge bosons, T-sigma S and T-pion P^a, $a = 1, 2, 3$ invariant under local SM symmetry group additional to the LσM Lagrangian (2.7) reads

$$\begin{aligned} \Delta\mathcal{L}_B &= D_\mu\bar{B}_a D^\mu B_a + \frac{1}{2}\,\mu_B^2\bar{B}B + \frac{1}{2}\,g_{\rm BB}(\bar{B}B)^2 \\ &+ g_{\rm BS}(S^2 + P^2)(\bar{B}B) + g_{\rm BH}(\mathcal{H}^\dagger\mathcal{H})(\bar{B}B) \\ &+ g_{\rm BP}(\bar{B}P)(BP)\,. \end{aligned} \tag{2.15}$$

After the EW and CS breaking, the first four terms in the scalar T-baryon potential give rise to the T-baryon mass term $m_{\rm B}\bar{B}B$, where

$$m_B^2 = -2\mu_B^2 - 2g_{\rm BS}u^2 - g_{\rm BH}v^2\,, \tag{2.16}$$

where, in general, $\mu_B^2 < 0$ and $g_{\rm BS}, g_{\rm BH}$ couplings can be positive or negative. In the nearly-conformal limit $|\mu_B| \ll u, v$, one notices that the T-baryon mass

$$m_B \gtrsim M_{\tilde{Q}} \sim u\,, \tag{2.17}$$

is naturally large in the TC decoupling limit $u \gg v$ and $g_{\rm BS} < 0$. In practice, one arrives at the model with five physical parameters controlling the properties of scalar T-baryons: the T-baryon mass scale $m_B \gtrsim \Lambda_{\rm TC} \sim 1$ TeV and four T-baryon–scalar dimensionless couplings $g_{{\rm B},i} \equiv \{g_{\rm BB}, g_{\rm BH}, g_{\rm BS}, g_{\rm BP}\}$. Remind, the masses of $\tilde{\pi}$, $\tilde{\sigma}$ and h bosons remain light and are placed at the EW scale in the heavy T-baryon limit under discussion [17], thus, validating the suggested scenario.

The meson-meson and baryon-meson interactions in ordinary QCD are usually very strong and non-perturbative i.e. the corresponding couplings are typically much larger than unity. Naively, this happens since the confinement scale is turned out to be comparable to the mass scale of pseudo-Goldstone modes in QCD. One sometimes refers to a very dense pion cloud surrounding nucleons as to a cause for such large nonperturbative couplings. In the case of relatively light (possibly, composite) Higgs boson and T-pions $m_{\tilde{\pi}} \sim 100 - 150$ GeV compared to a large T-confinement scale $\Lambda_{\rm TC} \gtrsim 1$ TeV, it may be more natural to expect a very different situation in T-hadron interactions – the T-pion cloud surrounding T-baryons is likely to be rather loose or sparse for $v/u \ll 1$ and $s_\theta \ll 1$. Thus, the T-hadron interactions at low energies may not be as intense as in QCD and the corresponding couplings should be smaller in this case although a more dedicated (e.g. lattice) analysis, of course, is necessary. The latter argument is in full agreement with the consistent small $h\tilde{\sigma}$-mixing limit mentioned above where the scalar self-couplings turn out to be small or even vanishing, and thus one expects the T-baryon–T-meson couplings to be small as well, i.e. $g_{{\rm B},i} \lesssim 1$.

The low-energy effective Lagrangian (2.15) appears to have an extra exact global $U(1)_{\rm TB}$ symmetry corresponding to the T-baryon number conservation in analogy to

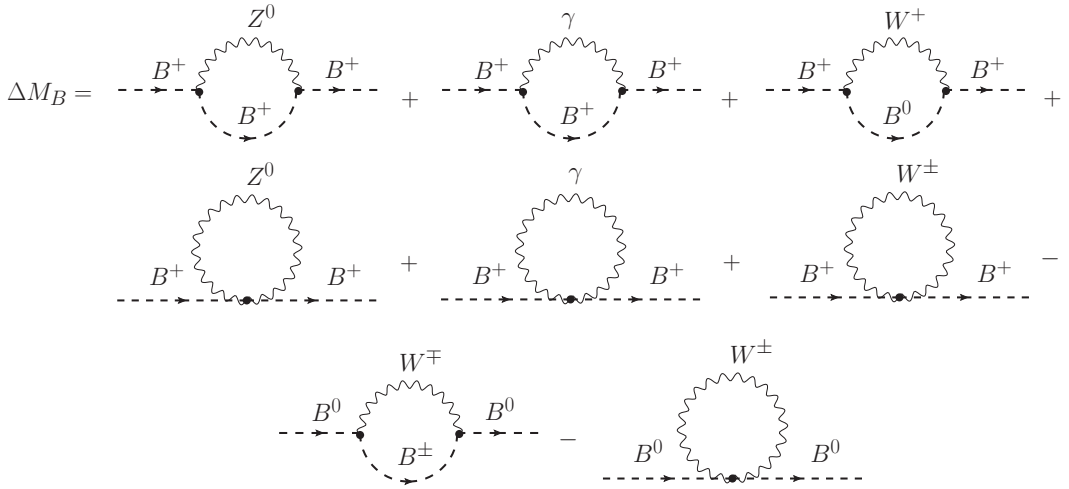

FIG. 2: Diagrams contributing to the EW mass splitting Δm_B in the scalar T-baryon spectrum.

ordinary baryon symmetry in the SM. Note, this symmetry has not been imposed forcefully. Instead, it emerged automatically due to the structure of T-baryon multiplet in the complex $SU(2)$-adjoint representation imposed by the chosen Dirac UV completion. In analogy to the usual baryon abundance, however, the present DM abundance may originate via generation of a sufficient T-baryon asymmetry e.g. by means of the well-known EW sphaleron mechanism at high energies in early Universe, in accordance to the popular ADM scenario [31, 33, 34].

The physical Lagrangian derived from Eq. (2.15) describes the T-baryon interactions with gauge $W^\pm, Z, \gamma$ bosons, scalar Higgs h and T-sigma $\tilde{\sigma}$ and T-pions $\tilde{\pi}^0, \tilde{\pi}^\pm$, as well as their self-interactions. The full expression is rather lengthy, and here we show the terms most relevant for T-baryon phenomenology only. In particular, the parameter-free gauge interactions critically important for possible T-baryon production mechanisms at the LHC and T-baryon scattering off nucleons are given by

$$\begin{aligned}\mathcal{L}_{\rm VB\bar{B}} &= ig\Big[W^-_\mu(B^0_{,\mu}\bar{B}^- - B^0\bar{B}^-_{,\mu} + \bar{B}^0_{,\mu}B^+ - \bar{B}^0 B^+_{,\mu}) \\ &+ (s_W A_\mu + c_W Z_\mu)(B^+_{,\mu}\bar{B}^+ + \bar{B}^-_{,\mu}B^-)\Big] + c.c.\,, \quad (2.18)\\ \mathcal{L}_{\rm VV B\bar{B}} &= g^2\Big[(\bar{B}^0 B^0 + \bar{B}^+ B^+)\, W^+_\mu W^{\mu -} \\ &+ \bar{B}^+ B^+ (s_W A_\mu + c_W Z_\mu)^2 - \bar{B}^+ B^- W^+_\mu W^{\mu +} \quad (2.19)\\ &- (\bar{B}^+ B^0 + \bar{B}^0 B^-)(s_W A_\mu + c_W Z_\mu) W^{\mu +}\Big] + c.c.\,,\end{aligned}$$

with the SM parameters g and θ_W fixed at the T-baryon mass scale $\mu = m_{\rm B}$ as a low-energy limit of the T-baryonic gauge form factors. Note, vector $\bar{B}^0 B^0 Z$-type couplings which determine the SI scattering of DM particles off nucleons at the Born level do not exist in this scenario. The scalar T-baryon–quark scattering, in fact, enters via an exchange by W-boson pair at one-loop level while the T-baryon–gluon scattering – at two-loop level with an intermediate charged T-baryon, and thus are strongly suppressed. The scalar T-baryon DM in this sense has a certain similarity to the electroweak-interacting DM scenario discussed e.g. in Ref. [38].

The scalar T-baryon annihilation processes in early Universe are largely dominated by effective T-baryon interactions with light composites ($\tilde{\sigma}$ and $\tilde{\pi}$) and the Higgs boson given by

$$\begin{aligned}\mathcal{L}_{\rm BS} &= \bar{B}B\big\{g_{\rm BS}\big[S_1^2 + 2uS_1 + P^2\big] + \frac{1}{2}\, g_{\rm BH}\big[S_2^2 + 2vS_2\big]\big\} \\ &+ g_{\rm BP}\big[\bar{B}^0 B^0 \tilde{\pi}^0\tilde{\pi}^0 + (\bar{B}^+ B^+ + \bar{B}^- B^-)\tilde{\pi}^+\tilde{\pi}^- \\ &+ (\bar{B}^-\tilde{\pi}^- + \bar{B}^+\tilde{\pi}^+)B^0\tilde{\pi}^0 + (B^+\tilde{\pi}^- + B^-\tilde{\pi}^+)\bar{B}^0\tilde{\pi}^0 \\ &+ \bar{B}^- B^+\tilde{\pi}^-\tilde{\pi}^- + \bar{B}^+ B^-\tilde{\pi}^+\tilde{\pi}^+\big]\,, \qquad (2.20)\end{aligned}$$

where $S_1 = hs_\theta + \tilde{\sigma}c_\theta$ and $S_2 = hc_\theta - \tilde{\sigma}s_\theta$. The latter Lagrangian is thus critical for the Higgs-induced tree-level elastic scattering of scalar T-baryons off nucleons in direct DM detection measurements as well as for the formation of the relic T-baryon abundance.

III. SCALAR T-BARYON DARK MATTER

A. T-baryon mass splitting

As was mentioned above, the T-baryon states in the strongly coupled $SU(2)_{\rm TC}$ theory are scalar composite di-T-quark states and can be rather heavy in the TC decoupling limit, $u \gg v$.

At temperatures above the EW phase transition scale but below the chiral symmetry breaking scale, $u \gg T \gtrsim v$, the UD state remains degenerate with other components of the $SU(2)$ triplet B^a. This is valid in the framework of considering low-energy effective theory where one-loop self-energies with virtual T-baryons, T-pions, Higgs boson and T-sigma are the same for B^0 and $B^\pm$

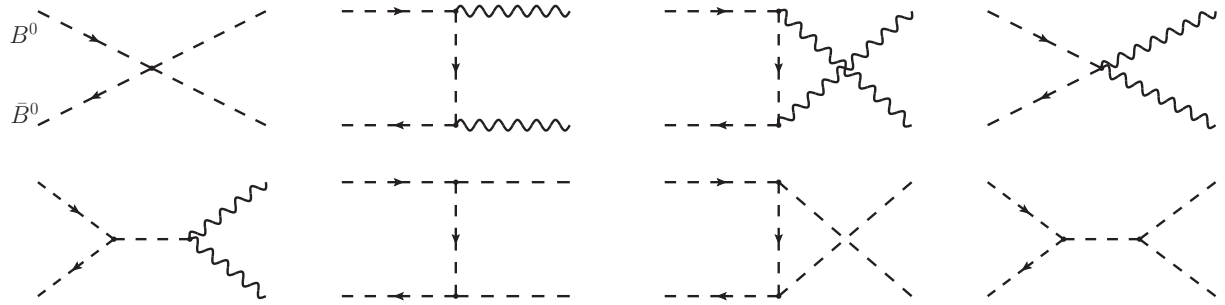

FIG. 3: Typical topologies for scalar T-baryon annihilation in the high-symmetry (HS) phase, $B^0\bar{B}^0 \to W^aW^b, \mathcal{H}\mathcal{H}$, SS, P_aP_b, $a,b = 1,2,3$ (upper row), and low-symmetry (LS) phase, $B^0\bar{B}^0 \to W^+W^-$, S_1S_2, where $S_{1,2} = \tilde{\pi}^{\pm,0}, \tilde{\sigma}, h$ (both upper and lower rows).

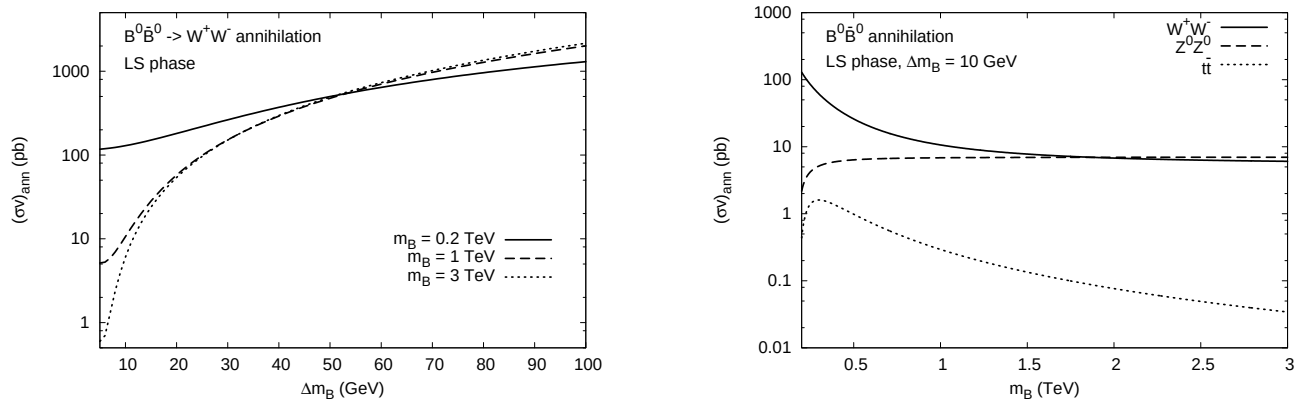

FIG. 4: The T-baryon LS annihilation cross section in the $B^0\bar{B}^0 \to W^+W^-$ channel as a function of the T-baryon mass splitting Δm_B (left) and the largest annihilation channels into SM final states $B^0\bar{B}^0 \to W^+W^-, Z^0Z^0, t\bar{t}$ as functions of the T-baryon mass scale m_B (right). In the left panel, the results are shown for three different mass scales $m_B = 0.2, 1, 3$ TeV, in the right panel the W^+W^- contribution is shown for $\Delta m_B = 10$ GeV. Here, $m_{\tilde{\pi}} = 150$ GeV and $\Delta m_{\tilde{\sigma}} = 20$ GeV are fixed.

and thus do not contribute to the mass splitting between neutral and charged T-baryons.

At lower temperatures, $T < v$, corresponding to the the EW-broken phase the di-T-quark state with zeroth electric charge UD is expected to be energetically favorable. Together with exact global T-baryon symmetry, the latter suggests that the neutral di-T-quark $B^0 \equiv UD$ state is also the lightest and thus stable. The mass splitting between B^0 and $B^\pm$ at low temperatures get well-defined contribution from the EW corrections depicted in Fig. 2. The latter are given by the one- and two-point self-energies with gauge bosons in the loop which are not cancelled in the mass difference according to Eqs. (2.18) and (2.19). The result for EW-induced mass splitting reads

$$\begin{aligned}\Delta m_B^{\rm EW} &= \frac{g_2^2 m_W^2}{16\pi^2 m_B}\Big\{\ln\Big(\frac{m_Z^2}{m_W^2}\Big) - \beta^2(\mu_Z)\ln(\mu_Z) + \beta^2(\mu_W)\ln(\mu_W) \\ &- \frac{4\beta^3(\mu_Z)}{\sqrt{\mu_Z}}\Big[\arctan\Big(\frac{\sqrt{\mu_Z}}{2\beta(\mu_Z)}\Big) + \arctan\Big(\frac{2-\mu_Z}{2\sqrt{\mu_Z}\beta(\mu_Z)}\Big)\Big] \\ &+ \frac{4\beta^3(\mu_W)}{\sqrt{\mu_W}}\Big[\arctan\Big(\frac{\sqrt{\mu_W}}{2\beta(\mu_W)}\Big) + \arctan\Big(\frac{2-\mu_W}{2\sqrt{\mu_W}\beta(\mu_W)}\Big)\Big]\Big\}, \end{aligned} \tag{3.1}$$

where $\mu_{Z/W} = m_{Z/W}^2/m_B^2$ and $\beta(x) = \sqrt{1-x^2/4}$. In the realistic limits, $\Delta m_B \ll m_B$ and $m_{Z/W} \ll m_B$, the

EW mass splitting may be estimated as

$$\Delta m_B^{\rm EW} \simeq \frac{g_2^2}{8\pi}\, m_W(1-c_W) \approx 0.17\,{\rm GeV}\,. \qquad (3.2)$$

Note, at the perturbative level the T-strong-induced mass splitting vanishes in both EW-unbroken and EW-broken phases in the considering model. However, in analogy to the di-quark spectrum QCD, one may discuss potentially large non-perturbative T-strong effects in the mass splitting in the chiral/EW symmetry broken phase. The situation is close to what we have in ordinary QCD when ud di-quark is split down in the di-quark mass spectrum by as much as ~ 70 MeV due to pion exchanges. Such non-perturbative effects, should be a proper subject for lattice studies and are not discussed here. In any case, the EW-induced splitting above (3.2) can be safely treated as a conservative lower bound. So for the sake of generality in our numerical analysis we consider the T-baryon DM implications in the EW-broken phase over the following wide range of allowed mass splittings:

$$\Delta m_B^{\rm EW} < \Delta m_B < M_{\rm EW} \sim 100\,{\rm GeV}\,,$$

while the basic qualitative conclusions will not strongly depend on the actual value of Δm_B.

B. Cosmological evolution

First, consider cosmological evolution of the T-baryon density in early Universe determined by the T-baryon annihilation processes. An assumption that the DM today consists mainly of scalar T-baryons provides with the upper limit on relic T-baryon abundance [39]

$$\Omega_{\rm TB} \lesssim \Omega_{\rm CDM} \simeq 0.2\Big[(\sigma v)^{\rm DM}_{\rm ann}/(\sigma v)^{\rm th}_{\rm ann}\Big]\,,$$
$$(\sigma v)^{\rm DM}_{\rm ann} \simeq 2.0\times 10^{-9}\ {\rm GeV}^{-2} \simeq 0.78\,{\rm pb}\,. \qquad (3.3)$$

The combined data from WMAP nine-year mission [40] suggest the value for present-day relic DM abundance $\Omega_{\rm CDM}h^2 = 0.1138 \pm 0.0045$. The expression (3.3) is then considered as a source for canonical constraints on TC model parameters and T-baryon asymmetry as long as a theoretical prediction for thermally averaged kinetic T-baryon annihilation cross section $(\sigma v)^{\rm th}_{\rm ann}$ is provided.

The irreversible T-baryon annihilation effectively starts at temperature $T_i \simeq m_B/3$. Depending on T_i, as well as on the T-baryon freeze-out temperature, $T_f \simeq m_B/20$, compared to the EW phase transition temperature, $T_{\rm EW} \sim M_{\rm EW} \sim 100$ GeV one may consider two limiting possibilities – the annihilation of T-baryons in the high ($T_f \gtrsim T_{\rm EW}$) and low ($T_i \lesssim T_{\rm EW}$) symmetry phases of the cosmological plasma (for more details on the characteristics of DM annihilation in these phases, see Ref. [18]).

Below the EWSB temperature, all heavier charged T-baryon $B^\pm$ and $\bar{B}^\pm$ states are expected to decay very quickly $B^\pm \to B^0 + W^\pm(\to l\bar{\nu}_l,\, q_i\bar{q}_j)$, and thus do not participate in annihilation processes. For example, the total leptonic $B^\pm$ 3-body decay width reads

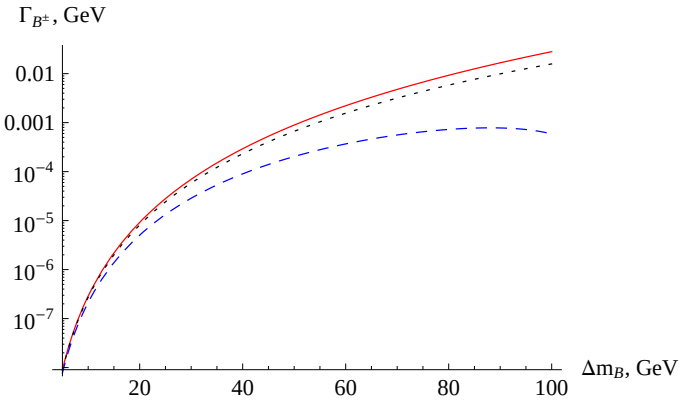

FIG. 5: Total decay width of charge T-baryons $B^\pm \to B^0 + W^\pm(\to l\bar{\nu}_l,\, q_i\bar{q}_j)$ as a function of the mass splitting Δm_B for different T-baryon mass scales $m_B = 100$ GeV (dashed), $m_B = 500$ GeV (dotted) and $m_B = 10$ TeV (solid).

$$\Gamma^{lept}_{B^\pm} = \sum_{l=e,\mu} \frac{g_2^4}{768\pi^3 m_W^4 m_\pm} \int_{m_l^2}^{(\Delta m_B)^2} \Big(1-\frac{m_l^2}{q^2}\Big) \times\ \bar{\lambda}(q^2, m_B^2, m_\pm^2) F(q^2) dq^2\,, \qquad (3.4)$$

where $\tau\nu_\tau$ channel does not contribute since $\Delta m_B < m_\tau$, and

$$F(q^2) = (m_\pm^2 - m_B^2)^2\Big(1+\frac{m_l^2}{q^2}-2\frac{m_l^4}{q^4}\Big) - q^2\big[2(m_\pm^2+m_B^2)-q^2\big]\Big(1-\frac{m_l^2}{2q^2}-\frac{m_l^4}{2q^4}\Big)\,,$$
$$\bar{\lambda}(a,b,c) = \Big(1-2\frac{a+b}{c}+\frac{(a-b)^2}{c^2}\Big)^{1/2}\,, \qquad (3.5)$$

and similarly for quark channels (additionally multiplied by the corresponding CKM matrix elements squared $|V_{ij}|^2$).

In the case of small mass splitting (3.2), the total $B^\pm \to B^0 + f_i\bar{f}_j$ decay width into light fermions is not practically sensitive to the T-baryon mass m_B, and is approximately equal to

$$\Gamma_{B^\pm} \simeq 1.7\times 10^{-16}\,{\rm GeV}\,, \qquad \Delta m_B = \Delta m_B^{\rm EW}\,.$$

which corresponds to the $B^\pm$ mean lifetime in the cosmological plasma, $\tau_B \simeq 3.8\times 10^{-9}$ s. This lifetime is larger than the Hubble time at the DM freeze-out, $\tau_f \equiv H^{-1}(T_f) \lesssim 10^{-10}$ s for $m_B \gtrsim 1$ TeV. This means that both neutral B^0 and $B^\pm$ components participate in the DM annihilation and such co-annihilation reactions as $B^0\bar{B}^\pm \to X$, $B^\mp\bar{B}^\pm \to X$ etc contribute to the formation of DM relic density. Given that the $SU(2)$ symmetry is nearly restored in the T-baryon sector in the limit $\Delta m_B \ll M_{\rm EW}$ and the decoupling limit $M_{\rm EW} \ll \Lambda_{\rm TC}$ is concerned, to a good approximation one could safely employ the T-baryon annihilation cross section $B^a\bar{B}^a \to X$ obtained in the EW unbroken phase (see below).

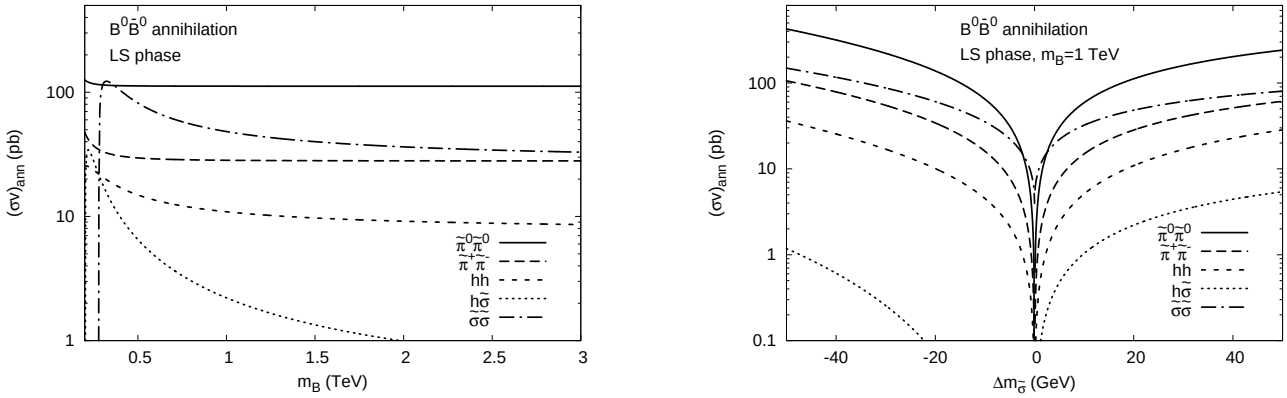

FIG. 6: The T-baryon LS annihilation cross sections in the (pseudo)scalar $B^0\bar{B}^0 \to \tilde{\pi}^0\tilde{\pi}^0, \tilde{\pi}^-\tilde{\pi}^-, hh, h\tilde{\sigma}, \tilde{\sigma}\tilde{\sigma}$ channels as functions of the T-baryon mass splitting m_B for fixed $\Delta m_{\tilde{\sigma}} = 20$ GeV (left) and $\Delta m_{\tilde{\sigma}} \equiv m_{\tilde{\sigma}} - \sqrt{3}m_{\tilde{\pi}}$ for fixed $m_B = 1$ TeV (right). Here, $m_{\tilde{\pi}} = 150$ GeV is fixed.

In the case of large mass splitting $\Delta m_B \gg m_{l,q}$, the partial $B^{\pm}$ decay widths into light fermions are not sensitive to the fermion masses $m_{l,q}$, and can be accounted for by a multiplicative factor in the total decay width $\Gamma_{B^{\pm}}$. The latter is shown in Fig. 5 as a function of $\Delta m_B = [10 \dots 100]$ GeV for three distinct T-baryon mass scales $m_B = 0.2$, 1, 10 TeV by dashed, dash-dotted and solid lines, respectively. There is a rather strong dependence of the decay rate on the T-baryon mass splitting, whereas almost no sensitivity is found w.r.t. the mass scale m_B variations. For TeV-mass T-baryons, it is straightforward to estimate the realistic mean lifetime of charge $B^{\pm}$ in the cosmological plasma $\tau_B = \Gamma^{-1}_{B^{\pm}} \sim 10^{-23} - 10^{-22}$ s for a realistic splitting $\Delta m_B \sim 100$ GeV which is about ten orders of magnitude smaller than the Hubble time in the beginning of DM annihilation epoch $H^{-1}(T_i) \sim 10^{-12}$ s. This means that at temperatures below T_i the charge T-baryons do not present in the plasma and, thus, no co-annihilation reactions $B^0\bar{B}^{\pm} \to X$, $B^{\mp}\bar{B}^{\pm} \to X$ etc contribute to the formation of DM relic density. So, only $B^0\bar{B}^0 \to X$ process should be considered which simplifies the subsequent calculations.

In analogy to ordinary baryons, the existence of a sufficient initial T-baryon asymmetry can be critical for a non-negligible amount of the scalar T-baryon DM in the case of large T-baryon–scalar couplings. So the T-baryon asymmetry appears to be an important parameter which completely determines the amount of such DM in the present Universe in the case of too fast annihilation rates. Various types of mixed (partially ADM) scenarios refer to an intermediate case of noticeable amounts of both particles and antiparticles although in not exactly equal amounts. A large existing freedom in the choice of T-baryon–scalar couplings $g_{\mathrm{B},i}$ makes it possible to consider both ADM and mixed DM scenarios. Below, for simplicity in our numerical analysis we consider a naive VLC scenario (in the near-conformal regime) where all the scalar self-couplings are equal to g_{TC}, i.e.

$$g_{\mathrm{B},i} = g_{\mathrm{TC}} = \frac{M_{\tilde{Q}}}{u}\,, \quad M_{\tilde{Q}} \simeq \frac{m_B}{2}\,, \tag{3.6}$$

which contains basics features of the general case. In this simplified scenario, m_B, $m_{\tilde{\pi}}$, and $\Delta m_{\tilde{\sigma}} \equiv m_{\tilde{\sigma}} - \sqrt{3}m_{\tilde{\pi}}$ are the only variable independent parameters.

Dominating topologies for EW and T-strong annihilation channels are shown in Fig. 3. In the *high-symmetry phase* (or HS phase) valid for heavy T-baryons $m_B \gtrsim 2$ TeV, the weak-induced T-baryon annihilation goes through the process $B^0\bar{B}^0 \to W_1W_1 + W_2W_2$ (with massless W^a) whose cross section reads

$$\sigma^{\mathrm{W,HS}}_{\mathrm{ann}} = \frac{2g_2^4}{\pi s\sqrt{1-\frac{4m_B^2}{s}}}\Big[\Big(5+\frac{4m_B^2}{s}\Big)\sqrt{1-\frac{4m_B^2}{s}} + \Big(1-\frac{6m_B^2}{s}+\frac{64m_B^4}{s^2}\Big)\ln\frac{1+\sqrt{1-\frac{4m_B^2}{s}}}{1-\sqrt{1-\frac{4m_B^2}{s}}}\Big]\,. \tag{3.7}$$

In the non-relativistic limit $v \ll 1$, however, the corresponding kinetic cross section

$$(\sigma v)^{\mathrm{W,HS}}_{\mathrm{ann}} \simeq \frac{13g_2^4}{2\pi m_B^2}\,v \tag{3.8}$$

vanishes. So, in this case the total annihilation cross section $(\sigma v)^{\mathrm{th}}_{\mathrm{ann}}$ which enter Eq. (3.3) will be essentially determined by the TC-induced $B^0\bar{B}^0 \to \mathcal{H}\mathcal{H}$, SS, P_aP_a channels (with massless final states), i.e.

$$(\sigma v)^{\mathrm{th}}_{\mathrm{ann}} \simeq (\sigma v)^{\mathrm{TC,HS}}_{\mathrm{ann}} \simeq \frac{g^2_{\mathrm{HS}}}{16\pi m_B^2}\,, \tag{3.9}$$

where

$$g^2_{\mathrm{HS}} = \frac{1}{4}g^2_{\mathrm{BH}} + 3g^2_{\mathrm{BS}} + (g_{\mathrm{BS}} + g_{\mathrm{BP}})^2\,.$$

Here, the diagrams with a single 4-particle vertex dominate, others are strongly suppressed by extra powers of m_B in propagators. Note, an inclusion of extra possible composites to the theory, e.g. in extended chiral symmetries and composite Higgs scenarios, as well as (pseudo)vector T-mesons may only increase the annihilation cross section.

It is worth to mention that the inequality (3.3), $\Omega_{\rm TB} \lesssim \Omega_{\rm CDM}$, applied for the T-baryon annihilation in the HS phase (3.9) imposes a constraint on the chiral symmetry breaking scale

$$u \gtrsim 4.3\,{\rm TeV} \gg v\,, \quad m_B \simeq 2u\,g_{\rm TC}\,, \tag{3.10}$$

which is valid under the naive scaling of the scalar self-couplings with the T-baryon mass (3.6). This constraint is consistent with the TC decoupling limit, and hence with the T-parameter constraint and the SM-like Higgs boson as discussed above in Sect. II A. Together with Eq. (3.10), the requirement for DM annihilation in the HS phase pushes up the T-baryon mass scale m_B

$$T_f \simeq \frac{m_B}{20} \gtrsim T_{\rm EW}\,, \quad m_B \gtrsim 2\,{\rm TeV}\,, \tag{3.11}$$

leading to a simple lower bound on scalar self-interaction rates

$$g_{{\rm B},i} = g_{\rm TC} \gtrsim g_{\rm TC}^{\rm min} \simeq \frac{1\,{\rm GeV}}{u}\,, \quad g_{\rm TC}^{\rm min} \lesssim 0.23\,. \tag{3.12}$$

Then, for the saturated inequality (3.3) when all the DM is made of the scalar T-baryons only, $\Omega_{\rm TB} \simeq \Omega_{\rm CDM}$, one obtains

$$g_{{\rm B},i} = g_{\rm TC} \gtrsim 0.23\,. \tag{3.13}$$

This bound is consistent with the initial hypothesis about the weakly-interacting heavy T-baryons in the TC decoupling limit $\Lambda_{\rm TC} \gtrsim 1\,{\rm TeV} \gg M_{\rm EW}$ formulated in Sect. II B. So, the heavy symmetric scalar T-baryon DM scenario with the relic abundance formation before the EW phase transition appears to be a feasible and appealing option. Of course, for a more precise quantitative analysis one would need to know the exact dependence of non-perturbative T-baryon couplings on T-sigma vev u (or, equivalently, on $\langle\bar{\tilde{Q}}\tilde{Q}\rangle$) going beyond the naive assumption (3.6) which is an important further subject for a lattice analysis (for a recent lattice study of effective Higgs–T-baryon interactions in $SU(4)$ gauge theory, see Ref. [32])

The T-baryon annihilation in the *low-symmetry phase* (or LS phase) $B^0\bar{B}^0 \to WW$ which should be relevant for not very heavy particles $m_B \lesssim 1$ TeV, the weak-induced annihilation rate qualitatively change its energy dependence such that it does not disappear close to the threshold any longer. In opposite, it becomes enhanced in the heavy T-baryon limit $m_B \gg m_W$, especially in the case of a large $B^0 - B^\pm$ mass splitting $\Delta m_B \gtrsim m_W$. This effect can be seen in Fig. 4(left), where the $B^0\bar{B}^0 \to WW$ cross section is shown as a function of $\Delta m_B = [5 \ldots 100]$ GeV for three different mass scale $m_B = 0.2, 1, 3$ TeV. Indeed, in the small $\Delta m_B \to 0$ limit one observes gross cancellations between the contact and t,u-channel contributions (s-channel terms are always suppressed) while at larger Δm_B the cancellations are less precise leading to such a characteristic shape of the cross section. We can immediately conclude from this result that the case of symmetric T-baryon DM which undergoes its annihilation mainly in the LS phase of the cosmological plasma can not be realized for large T-baryon mass splittings $\Delta m_B \gtrsim 10$ GeV and relatively light T-baryons $m_B < 2$ TeV. This is thus the particular version of ADM whose relic abundance is fully characterized by the initial T-baryon asymmetry providing a stable relic remnant of particles with the same T-baryon number and no strict constraints on T-baryon interaction rates analogical to that in the HS phase (3.13) can be drawn in this case.

In Fig. 4(right) the largest T-baryon annihilation cross sections into SM particles $WW, ZZ, t\bar{t}$ are shown as functions of the T-baryon mass scale $m_B = [0.2 \ldots 3]$ TeV. Here, only WW channel is sensitive to Δm_B which in the latter figure has been fixed to 10 GeV, for comparison.

The TC-induced annihilation channels into $h, \tilde{\sigma}, \tilde{\pi}$ final states approximately add up to

$$(\sigma v)_{\rm ann}^{\rm TC,LS} \;\simeq\; \frac{g_{\rm LS}^2}{16\pi m_B^2}\,, \tag{3.14}$$

altogether where in the case of large coupling $g_{\rm BS} \gg 1$ (or equivalently $m_B \gg u$) we have

$$\begin{aligned} g_{\rm LS}^2 \;&=\; \Big(1 - \frac{4m_h^2}{m_B^2}\Big)\Big(\frac{1}{2}g_{\rm BH}c_\theta^2 + g_{\rm BS}s_\theta^2\Big)^2 \\ &+\; \Big(1 - \frac{4m_{\tilde{\pi}}^2}{m_B^2}\Big)\big(2g_{\rm BS}^2 + (g_{\rm BS} + g_{\rm BP})^2\big) \\ &+\; \frac{1}{2}\bar{\lambda}(m_h^2, m_{\tilde{\sigma}}^2; m_B^2)(2g_{\rm BS} - g_{\rm BH})^2 s_\theta^2 c_\theta^2 \\ &+\; \Big(1 - \frac{4m_{\tilde{\sigma}}^2}{m_B^2}\Big)\Big(g_{\rm BS}c_\theta^2 + \frac{1}{2}g_{\rm BH}s_\theta^2\Big)^2\,, \end{aligned}$$

corresponding to the contact diagrams in Fig. 3 only. The exact result applicable also for the case of small effective couplings, e.g. $g_{\rm BS} \lesssim 1$, and hence for relatively light T-baryons $m_B \lesssim u$, is more complicated since it includes additional s,t,u-channel diagrams; it can be found in Appendix A. Note, in the small $h\tilde{\sigma}$-mixing limit $s_\theta \ll 1$, or $u \gg v$, and heavy T-baryon limit $m_B \gg u$, or $g_{\rm TC} \gg 1$,

$$g_{\rm LS} \simeq g_{\rm HS} \equiv g_{\rm eff}\,.$$

as expected.

The $B^0\bar{B}^0$ annihilation cross sections in the TC-induced (pseudo)scalar $\tilde{\pi}^0\tilde{\pi}^0, \tilde{\pi}^-\tilde{\pi}^-, hh, h\tilde{\sigma}, \tilde{\sigma}\tilde{\sigma}$ channels are presented in Fig. 6 as functions of the T-baryon mass scale m_B (left panel) and $\Delta m_{\tilde{\sigma}} \equiv m_{\tilde{\sigma}} - \sqrt{3}m_{\tilde{\pi}}$ (right panel). The m_B dependence flattens out at large m_B except for the $h\tilde{\sigma}$ channel since $g_{{\rm B},i} = g_{\rm TC} \sim m_B$ (c.f.

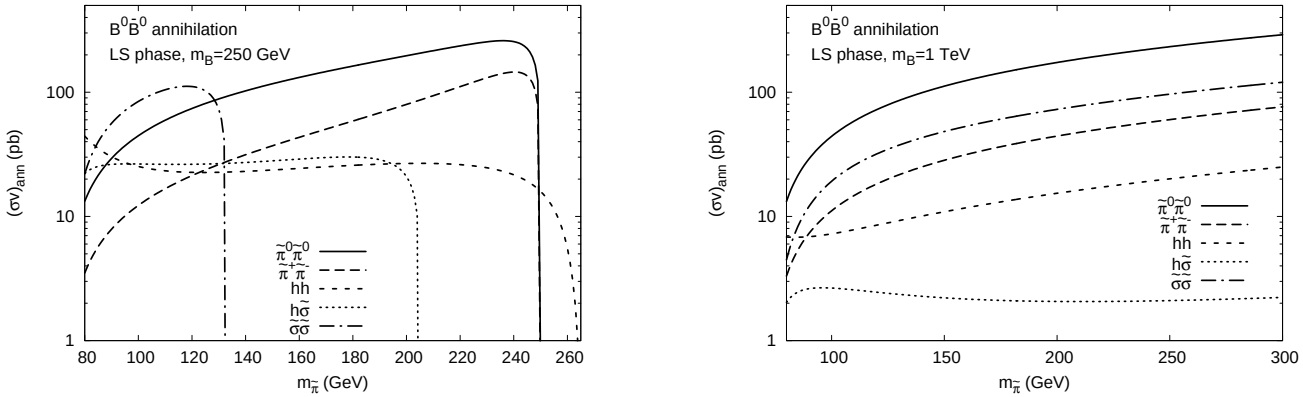

FIG. 7: The T-baryon LS annihilation cross sections in the (pseudo)scalar $B^0\bar{B}^0 \to \tilde{\pi}^0\tilde{\pi}^0, \tilde{\pi}^-\tilde{\pi}^-, hh, h\tilde{\sigma}, \tilde{\sigma}\tilde{\sigma}$ channels as functions of the T-pion mass $m_{\tilde{\pi}}$ for light $m_B = 250$ GeV (left) and heavy $m_B = 1$ TeV (right) T-baryons. Here, $\Delta m_{\tilde{\sigma}} = 20$ GeV is fixed.

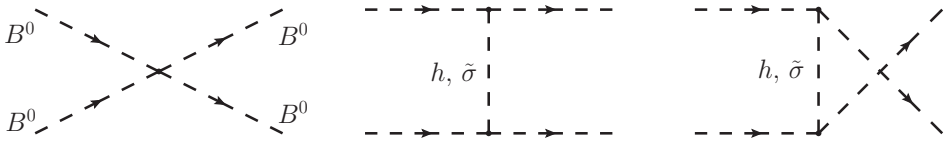

FIG. 8: Diagrams contributing to the elastic scattering of non-relativistic scalar T-baryons.

Eq. 3.6). In the TC decoupling limit $u \gg v$, corresponding to $s_\theta \ll 1$ and hence to $\Delta m_{\tilde{\sigma}} \to 0$, all the (pseudo)scalar annihilation channels vanish which is an important peculiarity of the considering scenario since $g_{\mathrm{B},i} = g_{\mathrm{TC}} \sim 1/u \to 0$ while there is no exact symmetry of the cross sections w.r.t. $\Delta m_{\tilde{\sigma}} \leftrightarrow -\Delta m_{\tilde{\sigma}}$. In Fig. 7 the same cross sections are plotted as functions of the T-pion mass $m_{\tilde{\pi}}$ for two different T-baryon mass values $m_B = 250$ GeV (left panel) and 1 TeV (right panel). Consequently, one finds a disappearance of the total TC-induced cross section in the heavy T-pion limit $m_{\tilde{\pi}} \gtrsim m_B$ which is otherwise peaked in intermediate regions.

It is worth to summarize that the total T-baryon annihilation rate is generally lower in the HS phase than that in the LS one not only by means of a higher T-baryon mass scale m_B, but also due to vanishing weak-induced contribution (3.8). In opposite, the weak-induced channels, especially into WW, appear to dominate the T-baryon annihilation cross section in the LS phase for a not too small T-baryon mass splitting. The bottom line of this study is that it is impossible to accommodate the symmetric T-baryon DM in the LS annihilation scenario unless the TC decoupling limit $\Delta m_{\tilde{\sigma}} \to 0$ and, simultaneously, the heavy T-baryon and low mass splitting limits are realized effectively approaching the HS annihilation scenario developed in Eqs. (3.7)–(3.13). Therefore, we encounter two rather different HS/LS annihilation scenarios which thus lead to symmetric/asymmetric T-baryon DM, respectively. The DM of an intermediate or mixed type can also be accommodated in the HS phase depending on the amount of initial T-baryon asymmetry.

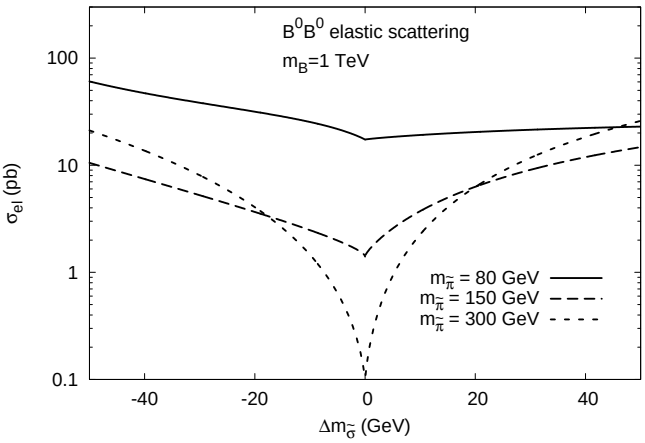

FIG. 9: The T-baryon elastic scattering cross section σ_{el} as a function of $\Delta m_{\tilde{\sigma}}$ for three different values of the T-pion mass $m_{\tilde{\pi}} = 80, 150$ and 300 GeV. Here, $m_B = 1$ TeV is fixed.

C. Elastic T-baryon scattering

One of the important inputs for the cosmogonic DM evolution and Structure Formation in late Universe is the elastic WIMP-WIMP scattering cross section. In the case of non-relativistic T-baryon DM, the elastic $B^0B^0 \to B^0B^0$ scattering is described by five diagrams – one contact diagram, two t-channel and corresponding cross (u-channel) diagrams via h and $\tilde{\sigma}$ exchanges shown

in Fig. 8. The non-relativistic T-baryon elastic scattering cross section is given by

$$\sigma_{el} \simeq \frac{G_{\rm B}^2}{32\pi m_B^2}\,,\ G_{\rm B} \equiv g_{\rm BB} + 8u^2 g_{\rm BS}^2\Big(\frac{c_\theta^2}{m_{\tilde\sigma}^2} + \frac{s_\theta^2}{m_h^2}\Big) \quad (3.15)$$

As a reference estimate, for $G_B \sim 1-10$ and 1 TeV T-baryon, one obtains $\sigma \sim 15\times(1-100)$ pb, respectively. In Fig. 9 the elastic cross section is illustrated as a function of $\Delta m_{\tilde\sigma}$ under the setting (3.6). So, the elastic T-baryon scattering appears to be weaker than usual elastic nucleon scattering but significantly stronger than DM particles' scattering in ordinary WIMP-based scenarios. Therefore, in fact we deal with a particular case of self-interacting DM which may be useful for DM astrophysics (see e.g. Ref. [41]).

IV. DARK MATTER DETECTION PROSPECTS

A. Indirect detection

At later stages of the Universe evolution, namely, after termination of T-baryon annihilation epoch, the T-baryon interactions are described by the effective low-energy Lagrangians (2.7) and (2.15) where the chiral and EW symmetries breaking should be performed according to Eqs. (2.9) and (2.10). In the case of *symmetric* T-baryon DM $m_B \gtrsim 2$ TeV, its late time LS annihilation is described by the cross sections shown in Figs. 4, 6 and 7. Here, one could distinguish two distinct cases: small $\Delta m_B < 10$ GeV and large $\Delta m_B > 10$ GeV T-baryon mass splitting.

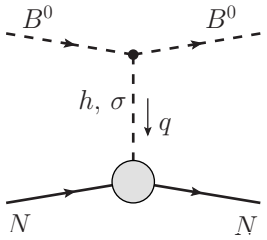

FIG. 10: The elastic scattering of neutral scalar T-baryon B^0 off a nucleon target N at tree level via h and σ exchanges in the t-channel relevant for direct DM detection close to the threshold $\sqrt{s_{\rm th}} \equiv m_B + m_N$.

In the first case, the $B^0\bar B^0 \to WW$ annihilation channel is suppressed, and WW, ZZ and $t\bar t$ channels altogether contribute at most ~ 10 pb or less to the total cross section, which is therefore dominated by T-strong channels for not too small $\Delta m_{\tilde\sigma} \gtrsim 5$ GeV, specifically, by

$$B^0\bar B^0 \to \tilde\pi^0\tilde\pi^0\,, \tilde\pi^-\tilde\pi^-\,, \tilde\sigma\tilde\sigma\,,$$

whose total contribution exceeds e.g. 100 pb for $m_B = 2$ TeV and $\Delta m_{\tilde\sigma} = 20$ GeV. Then, the dominant decay modes of T-sigma and T-pions with rather large (over 90 %) branching ratios in the considering 2-flavor $SU(2)_{\rm TC}$ VLC scenario are

$$\tilde\sigma \to \tilde\pi^{0,\pm}\tilde\pi^{0,\mp}\,, \quad \tilde\pi^0 \to Z\gamma\gamma\,, \quad \tilde\pi^\pm \to W^\pm\gamma\gamma\,,$$

respectively. We conclude that a key distinct indirect signature of the symmetric scalar T-baryon DM at a TeV mass scale will be its annihilation into predominantly light T-pions decaying into a vector boson and into two energetic photons which is a straightforward subject for a promising multi-GeV γ-lines search at FERMI [42]. Finally, in the very strong TC decoupling limit when $\Delta m_{\tilde\sigma} \ll 5$ GeV, the only $B^0\bar B^0 \to W^\pm W^\mp$ annihilation channel survives while the ZZ and $f\bar f$ ones vanish since the T-baryon–Higgs boson coupling is expected to decrease with the TC scale, e.g. $g_{\rm BH} \sim 1/u$ under the setting (3.6). The similar indirect observational consequences can be drawn for the T-baryon DM of a mixed type, with a lower density of particles and antiparticles capable of mutual annihilation, which may diminish corresponding detection rates. This situation means that even in the highly theoretically constrained VLC scenario, there is phenomenologically enough freedom to accommodate the heavy scalar symmetric T-baryon DM scenario predicting rather interesting and potentially detectable hard multi-γ signatures.

As was advocated in the previous section, if the T-baryon mass splitting is large $\Delta m_B > 10$ GeV and/or the mass scale is lower $m_B < 2$ TeV, one deals with the purely asymmetric T-baryon DM (other possibilities would be highly fine-tuned and are thus less likely). This is a pessimistic scenario for indirect DM detection measurements looking for T-baryon annihilation products – in the absence of a significant amount of anti-T-baryons and exact T-baryon conservation in present Universe, one does not expect to see any DM annihilation signatures. Only, direct ADM detection is relevant, so does in the symmetric DM case, considered above.

B. Direct detection

Consider now the scalar T-baryon implications for the direct DM detection experiments looking for nuclear recoils due to elastic non-relativistic WIMP-nucleon scattering. At *tree level*, the elastic scalar T-baryon–nucleon scattering is mediated by the scalar Higgs boson and T-sigma exchanges in the t-channel only as shown in Fig. 10.

Consider the consistent TC decoupling limit, $s_\theta \ll 1$. In this case, the elastic scattering of non-relativistic T-baryons off nucleons in an underground DM detector is dominated essentially by the Higgs boson exchange with a very small $q^2 \sim 1\,{\rm KeV}^2$. For such small q^2 values (slightly above the threshold $\sqrt{s_{\rm th}} \equiv m_B + m_N$) one deals the effective Higgs-nucleon form factor previously discussed in Ref. [43]. Then, the effective spin-independent

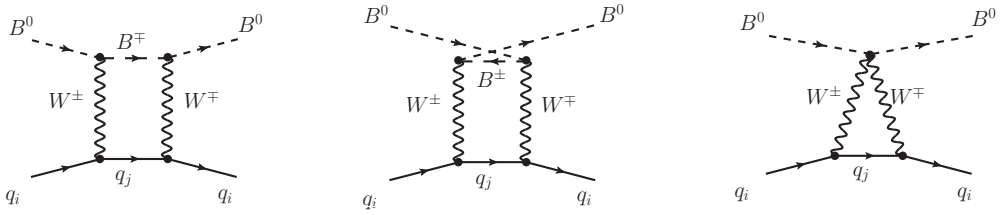

FIG. 11: The elastic scattering of neutral scalar T-baryon B^0 off a light quark target q_i at one loop level. Only the dominant topologies are shown.

T-baryon–nucleon elastic cross section reads

$$\sigma_{\rm SI}^{\rm nucl} \simeq \frac{\kappa^2}{\pi}\frac{m_N^4}{m_B^2 m_h^4}\,F_N^2 \simeq 5.45\,\kappa^2\Big(\frac{1\,\text{GeV}}{m_B}\Big)^2\cdot 10^{-38}\,\text{cm}^2\,, \qquad (4.1)$$

where m_N is the nucleon mass, and F_N parameterizes the effective tree-level matrix element for the Higgs interaction with the nucleon target incorporating the gluon anomaly [43, 44]

$$\frac{1}{v}\,\langle N|\sum_q m_q\bar{q}q|N\rangle \equiv F_N\,\frac{m_N}{v}\,\langle NN\rangle\,. \qquad (4.2)$$

In Eq. (4.1), we used the SM lattice result $F_N \simeq 0.375$ following the corresponding analysis of Ref. [45] where the uncertainty is dominated by the strange quark contribution, and κ is the effective T-baryon–Higgs coupling which in the generic VLC scenario reads

$$\mathcal{L}_{BBh} = \kappa v\, B\bar{B}h\,, \quad \kappa \simeq g_{\rm BH} + \frac{2m_h^2}{m_\sigma^2 - m_h^2}\,g_{\rm BS}\,.$$

At *one-loop level*, one encounters an appearance of gauge boson mediated contributions to the elastic T-baryon scattering off a quark in the nucleon target. Thus, it is meaningful to consider first the elementary $B^0q \to B^0q$ subprocess for such a short-range loop-induced reaction.

We have performed a dedicated analysis of the full one-loop order correction to the $B^0q \to B^0q$ ($q = u, d$) elastic cross section close to the corresponding threshold $\sqrt{s_{\rm th}}$. The dominant diagrams are shown in Fig. 11, while other possible topologies are found to be strongly suppressed. For this purpose, the effective Lagrangian of T-baryon interactions (2.15) together with the VLC model (2.7) has been implemented into the FeynRules framework [46] whose output was then used by FeynArts [47] to calculate the respective one-loop amplitudes. The latter were processed by the FormCalc package [48] into a Fortran code, together with necessary VLC parameter relations and mass formulae. The one-loop master integrals were evaluated by the LoopTools package [48], and the final cross section has been evaluated for relevant sets of physical parameters. Namely, the one-loop correction

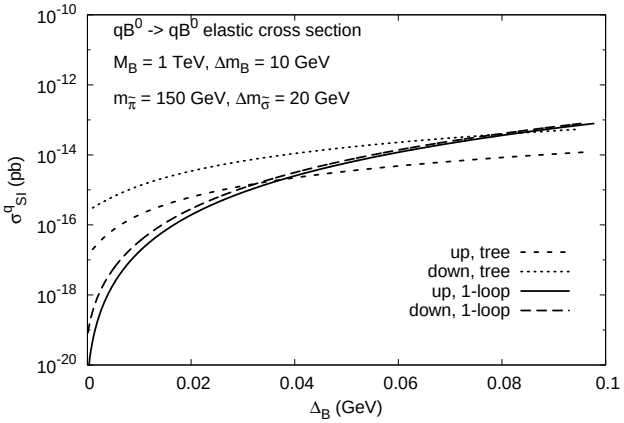

FIG. 12: The elastic T-baryon–quark scattering cross section of neutral scalar T-baryon B^0 off a light (u, d) quark target at one loop level as a function of Δ_B. The corresponding tree-level cross section is shown for comparison.

to the elastic $B^0q \to B^0q$ scattering cross section has been found as a function of

$$\Delta_B \equiv \sqrt{s} - \sqrt{s_{\rm th}} = \frac{2m_N}{m_B}\,E_B^{\rm lab}\,, \qquad (4.3)$$

where $E_B^{\rm lab} = m_B v^2/2$ ($v \sim 0.001$) is the T-baryon kinetic energy in the laboratory frame. The result shown in Fig. 12 clearly demonstrates a strong suppression of the one-loop correction compared to tree-level $B^0q \to B^0q$ scattering cross section in the non-relativistic scalar T-baryon limit, very close to the threshold. This is the case of thermal relic T-baryons in a Sun neighborhood. Namely, individual u and d quark scatterings at one loop level are found to be over three orders of magnitude smaller then the corresponding tree-level results. Therefore, the cross section given by t-channel Higgs boson exchange (4.1) is considered to be accurate enough and sufficient for a comparison to the DM direct experimental constraints. Note, for energetic T-baryons away from the threshold the one-loop induced cross section becomes large and dominate the elastic T-baryon scattering off a quark.

In Ref. [32], the effective scalar T-baryon–Higgs coupling has been constrained by lattice simulations in the strongly-coupled $SU(4)_{\rm TC}$ model. While a similar analy-

sis in the VLC model with confined $SU(2)_{\rm TC}$ symmetry yet has to be performed, in this first study we treat κ as a free parameter which can be constrained by the direct DM detection data, together with scalar T-baryon mass scale m_B. At the moment, the LUX experiment [37] provides the most stringent limit on $\sigma_{\rm SI}^{\rm nucl}$ (per nucleon in the case of a xenon target) which is roughly

$$-\log_{10}\left(\frac{\sigma_{\rm SI}^{\rm nucl}}{\rm cm^2}\right) \simeq 44.2 - 43.7\,,\;\; m_{\rm B} \simeq 0.5 - 2\,{\rm TeV} \quad (4.4)$$

providing the following bound on effective coupling

$$\kappa \lesssim 0.17 - 1.2\,, \quad (4.5)$$

respectively, and somewhat weaker constraints for larger m_B. This is in agreement with the lower bound on T-strong couplings from the heavy symmetric T-baryon constraint (3.13) and with our expectations for relatively weak T-baryon–T-meson interactions in the small $h\sigma$-mixing limit noticed above. Indeed, in Fig. 13 the recent LUX bound has been plotted vs T-baryon mass scale m_B together with the effective scalar T-baryon–nucleon SI cross section given by Eq. (4.1). The latter have been obtained for three distinct $\Delta m_{\tilde\sigma}$ values by using the naive scaling condition for scalar TC couplings (3.6). The cross section is less sensitive to the T-pion mass so it has been fixed to $m_{\tilde\pi} = 150$ GeV.

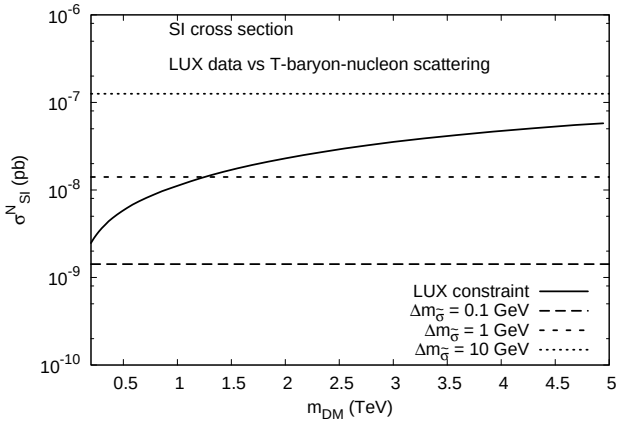

FIG. 13: The spin-independent T-baryon–nucleon cross section vs LUX constraint [37].

We note that the direct DM detection constraint from LUX in practice excludes large $\Delta m_{\tilde\sigma} \gtrsim 10$ GeV. It leaves the space only for a narrow a few GeV region in the vicinity of the TC decoupling limit $\Delta m_{\tilde\sigma}^{dec} \equiv 0$. Therefore, the direct DM constraint is complimentary to the corresponding constraints on $h\tilde\sigma$ mixing angle from the Higgs decays and from the T-parameter. It is worth to stress that the DM direct bound in Fig. 13 has turned out to be the most stringent constraint on new $SU(2)$ confined dynamics among other ones. Indeed, it pushes the acceptable $SU(2)_{\rm TC}$ scale $\Lambda_{\rm TC}$ even further away from the EW one (in a few TeV region) then the EW precision constraints. The bound (4.5) should be tested against lattice simulations in the considered strongly-coupled $SU(2)_{\rm TC}$ theory.

C. Collider signatures

The composite DM studies, and the new $SU(2)_{\rm TC}$ strong dynamics searches, in general, should be accompanied by respective scalar T-baryon searches at the LHC. In order to digest this possibility, let us briefly discuss the corresponding signatures of scalar T-baryon production in pp collisions at 14 TeV.

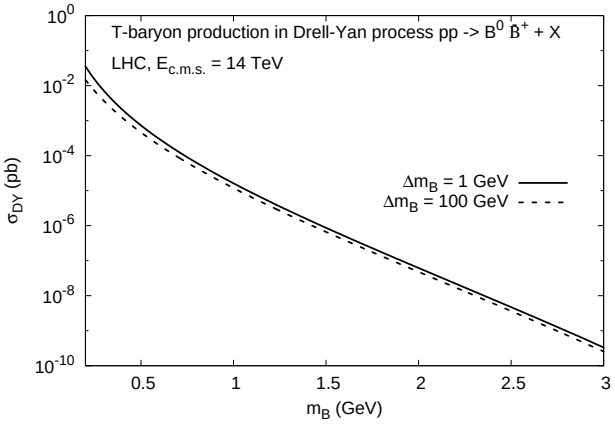

FIG. 14: The T-baryon $B^0\bar B^+$ pair production cross section via Drell-Yan channel in pp collisions at the LHC, $E_{c.m.s.} = 14$ TeV, for two distinct T-baryon mass splitting values, $\Delta m_B =$ 1 and 100 GeV.

One of the characteristic signals can be expected from the Drell-Yan charged-current reaction

$$q_i\bar q_j \to (W^\pm)^* \to B^0\bar B^\pm\,, \quad \bar B^\pm \to \bar B^0(W^\pm \to f_i\bar f_j)\,,$$

with deeply virtual W boson in the s channel. Here, heavy B^0 and $\bar B^0$ leave the detector unnoticed giving rise to a very large (a few TeV) missing mass in the missing E_T^{miss} spectrum, while the tagging on charged debris from the final W decay may be very problematic for a relatively small mass splitting $\Delta m_B \lesssim 50-70$ GeV. Also, this is due to a very dramatic dependence on the $B^\pm$ width on Δm_B shown in Fig. 5, such that at small Δm_B the charged $B^\pm$ "lives" longer before it decays into a W and invisible B^0 (a possibility for a displaced W emission accompanied by heavy invisibles). Note, the corresponding $B^0\bar B^\pm$ production cross section shown in Fig. 14 depends strongly on mass scale m_B only and does not depend on any other TC parameters and couplings, and only weakly depends on the T-baryon mass splitting Δm_B. Further more detailed studies of the T-baryon detection capabilities including realistic detector constraints should be performed elsewhere.

V. SUMMARY AND CONCLUSIONS

In this work, we have performed a detailed theoretical and phenomenological study of scalar T-baryon sector, in particular, with respect to its possible important role for DM astrophysics. The corresponding scenario of new gauge dynamics is based upon the consistent vector-like TC model with $SU(2)_{\rm TC}$ group which allows to obtain Dirac T-quarks in confinement from original chiral fermion multiplets. Starting from the phenomenological arguments provided by (i) EW precision tests and (ii) SM Higgs-like couplings, the T-baryon states turn out to be split and pushed up towards higher scales, away from the dynamical EW symmetry breaking scale (the TC decoupling limit, $\Lambda_{\rm TC} \gg M_{\rm EW} \sim 100$ GeV). In this regime, the scalar neutral T-baryon (T-diquark) $B^0 = UD$ state (the lightest among other T-diquarks) possessing a conserved quantum number can serve as an appealing DM candidate at a TeV mass scale, $m_B \gtrsim 0.5 - 1$ TeV. In the consistent TC decoupling limit, the scalar self-couplings of heavy T-baryons with light T-pions/T-sigma states are expected to decrease.

For $m_B > 2$ TeV one expects that the relic T-baryon abundance has been formed mainly before the EW phase transition. We have shown that in this case the total T-baryon annihilation cross section is rather weak and enables symmetric DM formation, whereas lighter T-baryons annihilating mostly in the low-symmetry phase of the cosmological plasma could only remain if there was a significant T-baryon asymmetry generation. A specific astrophysical signature of symmetric T-baryon DM is its annihilation into hard multi-γ final states via intermediate T-pion/T-sigma states, relevant for indirect DM detection measurements.

We have shown that the elastic T-baryon–quark scattering is induced at tree level by the Higgs/T-sigma bosons exchanges in the t-channel only, since the vector tree-level Z-boson is absent. We have calculated complete one-loop correction to the elastic scalar T-baryon scattering and found that it is strongly suppressed compared to the tree-level result. Most importantly, the direct DM detection constraints, e.g. those from LUX, on spin-independent elastic T-baryon–nucleon scattering cross section impose further ever stringent constraint on the T-baryon–Higgs coupling and hence on the chiral symmetry breaking scale. Namely, it imposes a much stronger suppression to the $h\tilde{\sigma}$ mixing angle (and hence the stronger hierarchy between the chiral and EW breaking scales) than the corresponding EW precision and SM Higgs bounds.

Finally, the search for heavy scalar T-baryons in the Drell-Yan production process with a trigger on a few TeV missing mass and, possibly, on accompanying W emission from a displaced vertex, is advised. A further more dedicated analysis of T-baryon implications at the LHC, in particular, in vector-boson fusion channels would be desirable.

Note, the question about compositeness of the light Higgs boson is not critical for cosmological evolution of the T-baryon DM analysis in the TC decoupling limit, $\Lambda_{\rm TC} \gg 100$ GeV, when the light technipion limit $m_{\tilde{\pi}} \ll \Lambda_{\rm TC}$ is concerned as long as scalar T-baryon–Higgs boson coupling is within the perturbative limit. Indeed, as we have advocated above in detail the couplings of heavy T-baryons with light composites (e.g. with pseudo-Goldstone states) are suppressed in the decoupling limit. As we have demonstrated above, the existing direct DM detection bounds set a limit on the T-baryon-Higgs boson coupling which should be understood as an important constraint on the existing variety of composite Higgs models. An account for the Higgs compositeness will not change this situation and, specifically, does not affect our basic conclusions neither for asymmetric, nor for symmetric DM scenarios. This is a motivation for the study of the cosmological T-baryon evolution independently on aspects of possible Higgs compositeness which will be thoroughly discussed in our forthcoming works. It is worth to stress here that the LUX experiment bound [37] in the TC decoupling limit is consistent with cosmological evolution and, in particular, with the freeze out of heavy T-baryons in the high-symmetry phase of the cosmological plasma setting an important stage for further development of composite DM scenarios in the TC decoupling limit.

An incorporation of the Sommerfeld enhancement effect into the cosmological evolution of scalar T-baryons could be a nice development of this work. However, in this first study we prefer not to incorporate this effect and hence to introduce an extra freedom into our analysis naively assuming a sharp cutoff in self-annihilation rates after the T-baryon freeze-out temperature. In fact, it is believed that the freeze out happens at relative velocities of about $v \sim 0.1 - 0.3$ where the Sommerfeld enhancement factor is of the order of unity for rather weak T-baryon-Higgs couplings suggested by both the TC decoupling limit and direct DM detection constraints. A proper analysis of the Sommerfeld enhancement effect could be a good point for further studies.

Acknowledgments

Stimulating discussions and helpful correspondence with Johan Bijnens, Johan Rathsman and Torbjörn Sjöstrand are acknowledged. V. B. and V. K. were partially supported by Southern Federal University grant No. 213.01-.2014/-013VG. R. P. is grateful to the "What is Dark Matter?" Program at Nordita (Stockholm) for support and hospitality during completion of this work. R. P. was supported in part by the Swedish Research Council, contract number 621-2013-428.

Appendix A: T-baryon annihilation into T-mesons

In Eq. (3.14) only contact diagrams dominating in the limit $m_B \gg u$ have been included. Here, we list the complete results for partial annihilation cross sections includ-

ing all diagrams in Fig. 3 and hence applicable for any hierarchy between m_B and u, m_h, $m_{\tilde\sigma}$. These read

$$(\sigma v)^{\rm XY,LS}_{\rm ann} \simeq \frac{g^2_{\rm XY}}{16\pi m_B^2}\,\bar\lambda(m_X^2, m_Y^2, m_B^2)\,, \qquad \text{(A1)}$$

where $\bar\lambda(a,b,c)$ is defined in Ref. (3.5), and effective couplings are

$$\begin{aligned}
g_{hh} &= \frac{1}{2}g_{\rm BH}c_\theta^2 + g_{\rm BS}s_\theta^2 \\
&+ \frac{2}{s-2m_h^2}\big(2u\,g_{\rm BS}s_\theta + v\,g_{\rm BH}c_\theta\big)^2 \\
&- \frac{g_{\tilde\sigma hh}}{s-m_{\tilde\sigma}^2}\big(2u\,g_{\rm BS}c_\theta - v\,g_{\rm BH}s_\theta\big) \\
&- \frac{g_{hhh}}{s-m_h^2}\big(2u\,g_{\rm BS}s_\theta + v\,g_{\rm BH}c_\theta\big)\,, \\
g_{\tilde\sigma\tilde\sigma} &= \frac{1}{2}g_{\rm BH}s_\theta^2 + g_{\rm BS}c_\theta^2 \\
&+ \frac{2}{s-2m_{\tilde\sigma}^2}\big(2u\,g_{\rm BS}c_\theta - v\,g_{\rm BH}s_\theta\big)^2 \\
&- \frac{g_{h\tilde\sigma\tilde\sigma}}{s-m_h^2}\big(2u\,g_{\rm BS}s_\theta + v\,g_{\rm BH}c_\theta\big) \\
&- \frac{g_{\tilde\sigma\tilde\sigma\tilde\sigma}}{s-m_{\tilde\sigma}^2}\big(2u\,g_{\rm BS}c_\theta - v\,g_{\rm BH}s_\theta\big)\,, \\
\sqrt{2}\,g_{\tilde\sigma h} &= (2g_{\rm BS} - g_{\rm BH})s_\theta c_\theta \\
&+ \frac{4(s-m_h^2-m_{\tilde\sigma}^2)}{(s-2m_h^2)(s-2m_{\tilde\sigma}^2)}\big(2u\,g_{\rm BS}s_\theta + v\,g_{\rm BH}c_\theta\big) \\
&\times \big(2u\,g_{\rm BS}c_\theta - v\,g_{\rm BH}s_\theta\big) \\
&- \frac{g_{h\tilde\sigma\tilde\sigma}}{s-m_{\tilde\sigma}^2}\big(2u\,g_{\rm BS}c_\theta - v\,g_{\rm BH}s_\theta\big) \\
&- \frac{g_{\tilde\sigma hh}}{s-m_h^2}\big(2u\,g_{\rm BS}s_\theta + v\,g_{\rm BH}c_\theta\big) \\
g_{\tilde\pi^0\tilde\pi^0} &= g_{\rm BS} + g_{\rm BP} - \frac{g_{\tilde\sigma\tilde\pi^0\tilde\pi^0}}{s-m_{\tilde\sigma}^2}\big(2u\,g_{\rm BS}c_\theta - v\,g_{\rm BH}s_\theta\big) \\
&- \frac{g_{h\tilde\pi^0\tilde\pi^0}}{s-m_h^2}\big(2u\,g_{\rm BS}s_\theta + v\,g_{\rm BH}c_\theta\big)\,, \\
\sqrt{2}\,g_{\tilde\pi^+\tilde\pi^-} &= 2g_{\rm BS} - \frac{g_{\tilde\sigma\tilde\pi^+\tilde\pi^-}}{s-m_{\tilde\sigma}^2}\big(2u\,g_{\rm BS}c_\theta - v\,g_{\rm BH}s_\theta\big) \\
&- \frac{g_{h\tilde\pi^+\tilde\pi^-}}{s-m_h^2}\big(2u\,g_{\rm BS}s_\theta + v\,g_{\rm BH}c_\theta\big)\,,
\end{aligned}$$

where $s \simeq 4m_B^2(1+v^2/4)$ close to the threshold $v \ll 1$.

[1] G. Aad *et al.* [ATLAS Collaboration], Phys. Lett. B **716**, 1 (2012) [arXiv:1207.7214 [hep-ex]].

[2] S. Chatrchyan *et al.* [CMS Collaboration], Phys. Lett. B **716**, 30 (2012) [arXiv:1207.7235 [hep-ex]].

[3] ATLAS Collaboration, ATLAS-CONF-2014-009 and ATLAS-CONF-2014-010, CERN Geneva, March 2014 ; S. Chatrchyan *et al.* [CMS Collaboration], arXiv:1401.6527 [hep-ex].

[4] S. Chatrchyan *et al.* [CMS Collaboration], JHEP **1306**, 081 (2013) [arXiv:1303.4571 [hep-ex]].

[5] S. Weinberg, Phys. Rev. **D13**, 974 (1976).

[6] L. Susskind, Phys. Rev. **D20**, 2619 (1979).

[7] S. Dimopoulos and L. Susskind, Nucl. Phys. **B155**, 237 (1979).

[8] E. Eichten and K. D. Lane, Phys. Lett. **B90**, 125 (1980).

[9] C. T. Hill and E. H. Simmons, Phys. Rept. **381**, 235 (2003) [Erratum-ibid. **390**, 553 (2004)] [hep-ph/0203079].

[10] F. Sannino, Acta Phys. Polon. B **40**, 3533 (2009).

[11] L. Vecchi, arXiv:1304.4579 [hep-ph].

[12] D. Barducci, A. Belyaev, M. S. Brown, S. De Curtis, S. Moretti and G. M. Pruna, JHEP **1309**, 047 (2013) [arXiv:1302.2371 [hep-ph]].

[13] A. De Simone, O. Matsedonskyi, R. Rattazzi and A. Wulzer, JHEP **1304**, 004 (2013) [arXiv:1211.5663

[hep-ph]].
[14] M. E. Peskin and T. Takeuchi, Phys. Rev. Lett. **65**, 964 (1990).
[15] M. E. Peskin, T. Takeuchi, Phys. Rev. D **46**, 381 (1992).
[16] C. Kilic, T. Okui and R. Sundrum, JHEP **1002**, 018 (2010) [arXiv:0906.0577 [hep-ph]].
[17] R. Pasechnik, V. Beylin, V. Kuksa and G. Vereshkov, Phys. Rev. D **88**, 075009 (2013) [arXiv:1304.2081 [hep-ph]].
[18] R. Pasechnik, V. Beylin, V. Kuksa and G. Vereshkov, Eur. Phys. J. C **74**, 2728 (2014) [arXiv:1308.6625 [hep-ph]].
[19] P. Lebiedowicz, R. Pasechnik and A. Szczurek, Nucl. Phys. B **881**, 288 (2014) [arXiv:1309.7300 [hep-ph]].
[20] A. Hietanen, R. Lewis, C. Pica and F. Sannino, arXiv:1404.2794 [hep-lat].
[21] G. Cacciapaglia and F. Sannino, arXiv:1402.0233 [hep-ph].
[22] M. R. Buckley and E. T. Neil, Phys. Rev. D **87**, no. 4, 043510 (2013) [arXiv:1209.6054 [hep-ph]].
[23] S. Nussinov, Phys. Lett. B **165**, 55 (1985);
S. M. Barr, R. S. Chivukula, and E. Farhi, Phys. Lett. B **241**, 387 (1990).
[24] S. B. Gudnason, C. Kouvaris and F. Sannino, Phys. Rev. D **74**, 095008 (2006) [hep-ph/0608055].
[25] S. B. Gudnason, C. Kouvaris and F. Sannino, Phys. Rev. D **73**, 115003 (2006) [hep-ph/0603014].
[26] M. Y. Khlopov and C. Kouvaris, Phys. Rev. D **78**, 065040 (2008) [arXiv:0806.1191 [astro-ph]].
[27] M. Y. Khlopov, A. G. Mayorov and E. Y. Soldatov, Int. J. Mod. Phys. D **19**, 1385 (2010) [arXiv:1003.1144 [astro-ph.CO]].
[28] E. Del Nobile and F. Sannino, Int. J. Mod. Phys. A **27**, 1250065 (2012) [arXiv:1102.3116 [hep-ph]].
[29] F. Sannino, Acta Phys. Polon. B **40**, 3533 (2009) [arXiv:0911.0931 [hep-ph]].
[30] T. A. Ryttov and F. Sannino, Phys. Rev. D **78**, 115010 (2008) [arXiv:0809.0713 [hep-ph]].
[31] R. Lewis, C. Pica and F. Sannino, Phys. Rev. D **85**, 014504 (2012) [arXiv:1109.3513 [hep-ph]].
[32] T. Appelquist, E. Berkowitz, R. C. Brower, M. I. Buchoff, G. T. Fleming, J. Kiskis, G. D. Kribs and M. Lin *et al.*, arXiv:1402.6656 [hep-lat].
[33] A. Belyaev, M. T. Frandsen, S. Sarkar and F. Sannino, Phys. Rev. D **83**, 015007 (2011) [arXiv:1007.4839 [hep-ph]].
[34] K. Petraki and R. R. Volkas, arXiv:1305.4939 [hep-ph].
[35] C. Kouvaris, Phys. Rev. D **88**, no. 1, 015001 (2013) [arXiv:1304.7476 [hep-ph]].
[36] E. Aprile *et al.* [XENON100 Collaboration], Phys. Rev. Lett. **109**, 181301 (2012) [arXiv:1207.5988 [astro-ph.CO]].
[37] D. S. Akerib *et al.* [LUX Collaboration], Phys. Rev. Lett. **112**, 091303 (2014) [arXiv:1310.8214 [astro-ph.CO]].
[38] J. Hisano, K. Ishiwata, N. Nagata and T. Takesako, JHEP **1107**, 005 (2011) [arXiv:1104.0228 [hep-ph]].
[39] G. Steigman, B. Dasgupta and J. F. Beacom, Phys. Rev. D **86**, 023506 (2012) [arXiv:1204.3622 [hep-ph]].
[40] G. Hinshaw *et al.* [WMAP Collaboration], Astrophys. J. Suppl. **208**, 19 (2013) [arXiv:1212.5226 [astro-ph.CO]].
[41] D. N. Spergel and P. J. Steinhardt, Phys. Rev. Lett. **84**, 3760 (2000) [astro-ph/9909386].
[42] M. Ackermann *et al.* [Fermi-LAT Collaboration], Phys. Rev. D **88**, 082002 (2013) [arXiv:1305.5597 [astro-ph.HE]].
[43] M. A. Shifman, A. I. Vainshtein and V. I. Zakharov, Phys. Lett. B **78**, 443 (1978).
[44] J. Giedt, A. W. Thomas and R. D. Young, Phys. Rev. Lett. **103**, 201802 (2009) [arXiv:0907.4177 [hep-ph]].
[45] R. J. Hill and M. P. Solon, Phys. Lett. B **707**, 539 (2012) [arXiv:1111.0016 [hep-ph]].
[46] A. Alloul, N. D. Christensen, C. Degrande, C. Duhr and B. Fuks, Comput. Phys. Commun. **185**, 2250 (2014) [arXiv:1310.1921 [hep-ph]].
[47] T. Hahn, Comput. Phys. Commun. **140**, 418 (2001) [hep-ph/0012260].
[48] T. Hahn and M. Perez-Victoria, Comput. Phys. Commun. **118**, 153 (1999) [hep-ph/9807565].